POLITECNICO DI TORINO

MASTER's Degree in Mechatronic Engineering

MASTER's Degree Thesis

Hardware and software platforms for IEEE 802.11p and C-V2X coexistence

Supervisors

Prof. Claudio Ettore CASETTI

Francesco RAVIGLIONE

Marco RAPELLI

Giuseppe PERRONE

Candidate

Stefano ALLUCI

March 2026

Hardware and software platforms for IEEE 802.11p and C-V2X coexistence

Alluci Stefano

Abstract

In recent years, two main technologies have emerged and have hit the market for vehicular communication: one belonging to the Wi-Fi family, based on IEEE 802.11p, and the other built on cellular networks and standardized by 3GPP starting from Release 14, commonly referred to as Cellular-V2X (C-V2X). The automotive industry is currently experiencing a phase of uncertainty due to the lack of clear regulations regarding which standards and technologies should be adopted for vehicular communications. While the United States appears to favor C-V2X, following the FCC's latest Report and Order, which reserves only the last three channels of the 5.9 GHz band exclusively for C-V2X use, Europe has adopted a technology-neutral stance. For example, Volkswagen has already deployed an IEEE 802.11p-based system for vehicular communication. Consequently, in the near future, particularly in Europe, both C-V2X and DSRC (IEEE 802.11p) technologies are expected to be implemented in vehicles. In order to effectively address this scenario, it is essential to conduct a realistic coexistence study between these two technologies, especially as they use the same frequency spectrum dedicated to Intelligent Transport Systems (ITS). This thesis focuses on such a study, using packet loss and message latency as primary performance metrics. More specifically, the evaluation of latency is based on IVIM (Infrastructure to Vehicle Information Message) transmissions. Due to hardware synchronization limitations, latency is assessed through the measurement of Round Trip Time (RTT), supported by an estimation of the message handling time at the application layer. The comparison of RTT performance between IEEE 802.11p and C-V2X transmissions is carried out under both congested and non-congested network conditions, considering as a reference the LTE-V2X Release 14 technology. This approach enables a comprehensive and realistic assessment of the behavior of the two technologies in coexistence scenarios, providing valuable insights into their performance and interaction in future mixed vehicular communication environments.

Table of Contents

List of Figures

List of Tables

Acronyms

ABS	Anti-lock Braking Systems.
ACs	Access Categories.
ADAS	dvanced Driver-Assistance Systems.
AEB	Automatic Emergency Braking.
AIFS	Arbitration Interframe Spaces.
ASN.1	Abstract Syntax Notation One ASN.1.
AVP	Autonomous Vehicle Platooning.
AVL	Automatic Vehicle Location.
BE	Best Effort.
BK	Background.
BSS	Basic Service Set.
BTP	Basic Transport Protocol.
BTP-SAP	BTP Service Access Point.
CAD	Cooperative Automated Driving.
CAM	Cooperative Awareness Messag.
CBR	Channel Busy Ratio.
CCA	Clear Channel Assessment.
CCH	Control Channel.
CCWS	Cooperative Collision Warning Systems.
CEPT	European Conference of Postal and Telecommunications Administrations.
C-ITS	Cooperative Intelligent Transport Systems.
CPS	contiguous partial sensing.
CPM	Cooperative Perception Messag.
C-V2X	Cellular-V2X.
CW	Contention Window.
DCM	Dual Carrier Modulation.
D2D	Device-to-Device.
DCC	Decentralized Congestion Control.
DENM	Decentralized Environmental Notification Message.

DIFS	Distributed Coordination Function Interframe Space.
DL	downlink.
DSRC	Dedicated Short Range Communication.
EARFCN	E-UTRA Absolute Radio Frequency Channel Number.
EDCA	Enhanced Distributed Channel Access.
ETSI	European Telecommunications Standards Institute.
FCC	Federal Communications Commissio.
FEC	Forward Error Correction.
FCW	Forward Collision Warning.
GLC	Geographic Location Container.
GN	GeoNetworking.
GNSS	Global Navigation Satellite System.
ICI	inter-carrier interference.
ICT	information and communication technologies.
IEEE	Institute of Electrical and Electronics Engineers.
ISI	inter-symbol interference.
ITS	Intelligent Transport Systems.
ITS BSA	ITS Basic Set of Applications.
IVIM	Infrastructure to Vehicle Information Messag.
LaTe	Latency Tester.
LBS	Location-Based Services.
LDM	Local Dynamic Map.
LLC	Logical Link Control.
LTE	Long Term Evolution.
MAC	Medium Access Control.
MANET	Mobile Ad-Hoc Network.
MCS	Modulation and Coding Scheme.
MEC	Multi-access Edge Computing.
MLC	Map Location Container.
NTP	Network Time Protocol.
OBU	On Board Units.
OCB	Outside the Context of a Basic Service Set.
OFDM	Orthogonal Frequency-Division Multiplexing.

PBPS	periodic-based partial sensing.
PER	Packet Error Rate.
PHY	Physical.
PL	Platoon Leader.
PMs	Platoon Members.
PPPP	ProSe Per Packet Priority.
PPS	Pulse-Per-Second.
PRR	Packet Reception Ratio.
ProSe	Proximity Service.
PSCCH	Physical Sidelink Control Channel.
PSSCH	Physical Sidelink Shared Channel.
RAN	Radio Access Network.
RBs	Resource Blocks.
RC	Reselection Counter.
RRI	Resource Reservation Interval.
RSU	Road Side Units.
RSSI	Received Signal Strength Indicator.
RTC	Real-Time Clock.
RTK	Real-Time Kinematics.
RTT	Round Trip Time.
SAE	Society of Automotive Engineer).
SAEM	Services Announcement Essential Message.
SC-FDMA	Single-Carrier Frequency Division Multiple Access.
SCI	Sidelink Control Information.
SCH	Service Channels.
SIFS	Short Interframe Space.
SL	sidelink.
SPS	Semi-Persistent Scheduling.
SW	Selection Window.
TBs	Transport Blocks.
TSB	Topologically-Scoped Broadcast.
UEs	User Equipments.
UL	uplink.
UPER	Unaligned Packed Encoding Rules.
UPs	User Priorities.
V2I	Vehicle-to-Infrastructure.
V2N	Vehicle-to-Network.

V2P	Vehicle-to-Pedestrian.
V2V	Vehicle-to-Vehicle.
V2X	Vehicle-to-Everything.
VAM	Vulnerable Road Users Awareness Message.
VANETs	Vehicular Ad-Hoc Networks.
VI	Video.
VO	Voice.
WAVE	Wireless Access in Vehicular Environments.
WSAs	WAVE Service Advertisements.

Chapter 1

Introduction

In recent years, vehicle technologies have evolved rapidly, aiming to provide higher levels of automation and increasingly advanced centralized and decentralized services. The journey toward vehicle automation began with the introduction of Advanced Driver-Assistance Systems (ADAS) in the 1970s, marked by the first implementation of Anti-lock Braking Systems (ABS) approximately 50 years ago [1]. In the following years, more advanced systems were developed, and divided according to the SAE (Society of Automotive Engineer) taxonomy [2]:

- **Level 0:** No Driving Automation
- **Level 1:** Driver Assistance
- **Level 2:** Partial Driving Automation
- **Level 3:** Conditional Driving Automation
- **Level 4:** High Driving Automation
- **Level 5:** Full Driving Automation

Level 0 ADAS systems do not perform any vehicle control functions; rather, they provide information to the driver and assist in monitoring both the surrounding environment and the driver's condition. Examples include Parking Sensors and Forward Collision Warning (FCW) systems. Level 1 and Level 2 ADAS systems still leave overall control to the driver but can manage specific driving functions through dedicated actuators. Level 1 systems control individual functions in specific situations. For example, Automatic Emergency Braking (AEB) differs from FCW in that it can autonomously apply the brakes if the driver fails to respond to a collision warning, whereas FCW only provides visual and acoustic alerts. In this sense, AEB represents an active extension of FCW[1]. Level 2 systems retain the same level of driver authority but can execute more complex maneuvers, Autonomous Parking ADAS assists the driver in locating and entering a parking space, managing steering while the driver maintains supervision or pedal control.[1]. The capabilities of ADAS systems are limited by their underlying technology. Sensors and cameras may fail to detect hazardous situations in blind spots and typically operate within a restricted

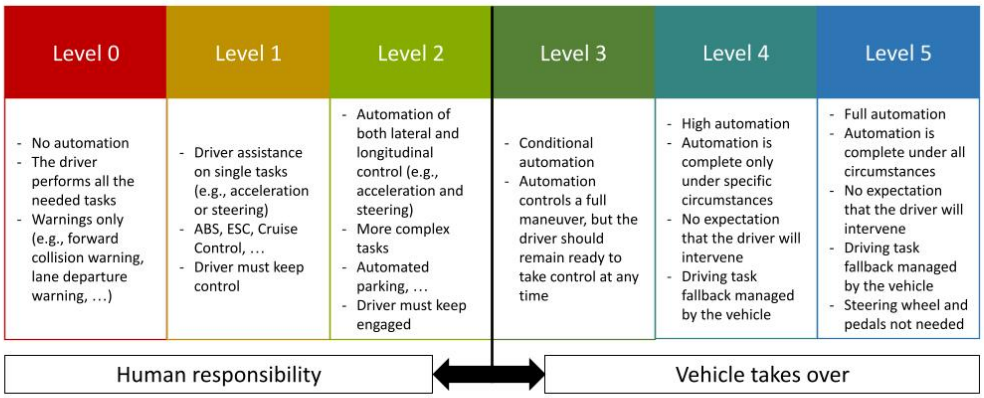

Figure 1.1: SAE Automation Levels, from [3]

range. Starting from SAE Level 3 and above, information redundancy and vehicle connectivity become increasingly critical, leading to the emergence of Intelligent Transport Systems (ITS).

An ITS can be defined as any system that employs communication technologies and information processing to enhance safety, mobility, and the overall efficiency of transportation infrastructure[4]. The European Telecommunications Standards Institute (ETSI) has developed standards for connected vehicles, focusing on communication protocols, services, and development frameworks. It is therefore possible to identify three evolutionary phases:

- **Day 1:** Awareness
- **Day 2:** Collective Perception
- **Day 3:** Coordinated Maneuvers

During Day 1, vehicles share basic positional information. The Collective Perception phase involves exchanging sensed data, allowing Road Side Units (RSUs) and On Board Units (OBUs) to share their perception of the environment. This approach mitigates blind-spot limitations of ADAS systems through Cooperative Collision Warning Systems (CCWS), in which ITS nodes continuously exchange information [5]. Autonomous Vehicle Platooning (AVP) represents an example of a Coordinated Maneuver system. It is an effective solution for reducing traffic congestion, energy consumption, and emissions. In a platoon, vehicles travel in close formation under the supervision of a Platoon Leader (PL), who coordinates the actions of the Platoon

Members (PMs). While early platooning approaches were limited to homogeneous vehicle groups, ongoing research has enabled dynamic platoons, allowing heterogeneous vehicles to join or leave the formation in real time[6]. Achieving such coordination requires dedicated communication networks, namely Vehicular Ad-Hoc Networks (VANETs), a specialized type of Mobile Ad-Hoc Network (MANET). The integration of information and communication technologies (ICT), sensing systems, and wireless communication enables the development of a safer, more efficient, and fully connected transportation ecosystem. However, this vision presents significant technical challenges, particularly due to high vehicle mobility, intermittent connectivity, stringent latency requirements, and environmental variability [7].

Dedicated standards have led to the development of a wide range of applications that enable wirelessc data exchange between vehicles and their surroundings, commonly referred to as Vehicle-to-Everything (V2X) communications. Depending on the specific area of application, V2X technologies can be divided into several , as defined by 3GP. According to 3GPP[8].V2X technologies can be categorized as follows:

- Vehicle-to-Vehicle (V2V): communication between vehicles
- Vehicle-to-Infrastructure (V2I): communication between vehicles and RSUs
- Vehicle-to-Pedestrian (V2P): communication between vehicles and vulnerable road users (VRUs), typically via smartphones
- Vehicle-to-Network (V2N): communication between vehicles and broader network services

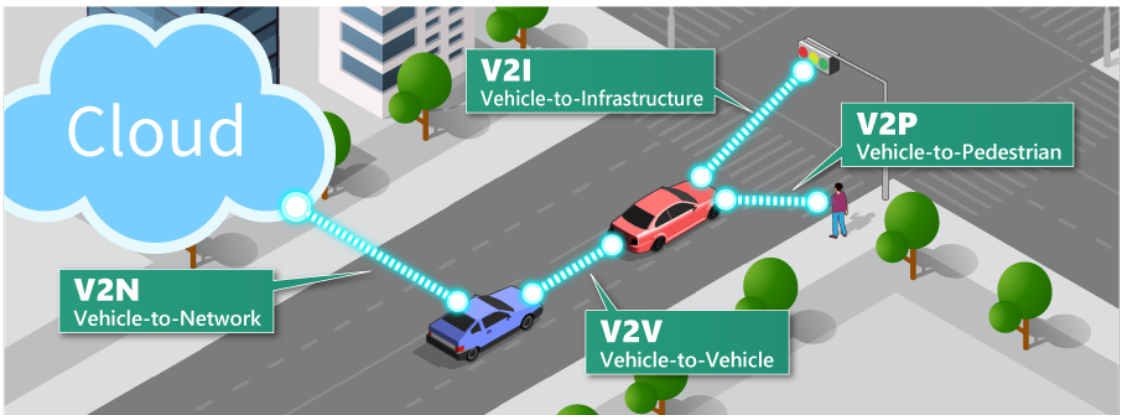

Figure 1.2: Scheme showing the most common sub-use cases of V2X communication: Vehicle-to-Vehicle (V2V), Vehicle-to-Infrastructure (V2I), Vehicle-to-Network (V2N) and Vehicle-to-Pedestrian (V2P).

It therefore becomes crucial to develop, deploy, and evaluate different technologies for both V2V and V2I communication, possibly integrating multiple standards to enhance vehicular communication capabilities. The Institute of Electrical and Electronics Engineers (IEEE) and ETSI are the primary standardization bodies in

vehicular communications. Both ETSI ITS-G5 and IEEE Wireless Access in Vehicular Environments (WAVE) are based on Dedicated Short Range Communication (DSRC), a Wi-Fi-based technology specifically designed for vehicular environments. As an alternative solution, Cellular-V2X (C-V2X) was proposed by 3GPP, leveraging Long Term Evolution (LTE) and 5G technologies. NR-V2X further extends C-V2X capabilities by introducing advanced resource allocation mechanisms.To achieve the ultimate objective of Intelligent Transport Systems, the so called autonomous coordinated maneuvers, all nodes within VANETs must be interconnected. In such scenarios, channel congestion becomes a critical issue. This thesis focuses on the study of the coexistence of the two technologies, C-V2X and DSRC, in both free-flow and congested environments.

Chapter 2

Communication for connected vehicles

The success of Intelligent Transportation System (ITS) applications strongly depends on reliable and efficient inter-vehicular communication. As previously discussed, Vehicular Ad Hoc Networks (VANETs) were introduced as a specialized evolution of Mobile Ad Hoc Networks (MANETs), specifically designed to address the unique characteristics of vehicular environments. These characteristics include extremely dynamic network topologies caused by high vehicle mobility, rapidly varying link conditions, and the requirement to guarantee ultra-low latency even under fluctuating traffic loads. V2X communication, whether based on C-V2X or DSRC technology, occurs between vehicles and Roadside Units (RSUs). Vehicles must be equipped with an appropriate radio interface, commonly referred to as an On-Board Unit (OBU), which enables the formation of short-range wireless ad hoc networks. In addition, vehicles require positioning hardware capable of providing accurate location information, typically through a Global Navigation Satellite System (GNSS) receiver (e.g., GPS or differential GNSS techniques). Fixed RSUs, which are connected to the backbone network, play a fundamental role in supporting communication services. Their deployment strategy is a critical design aspect and varies depending on the specific applications, coverage requirements, and communication protocols adopted. In this context, the need to further reduce latency and enhance service reliability has driven the adoption of Multi-access Edge Computing (MEC). MEC is a paradigm that brings computing and storage resources closer to the edge of the Radio Access Network (RAN). Its primary objective is to provide cloud capabilities in close proximity to mobile users, thereby reducing network congestion and, most importantly, significantly lowering end-to-end latency. With the introduction of 5G systems, extremely stringent performance requirements have emerged, including ultra-low service latency (below 5 ms) [9]. Traditional cloud computing architectures, which rely on remote data centers, are generally unable to meet such requirements due to the long communication paths through the core network. MEC addresses this limitation by relocating computational resources closer to end users, for instance at an eNB or gNB, at aggregation points, small cell gateways, or even Wi-Fi access

points. This architectural shift provides several advantages. First, latency is reduced because traffic can be processed locally, without traversing the entire core network or reaching distant cloud servers. The reduction in propagation and processing delays along the communication path results in substantial latency gains. Second, by moving processing, caching, and storage functions to the network edge, MEC limits the continuous flow of high-volume data toward the core network. Consequently, MEC offers significant improvements in both latency performance and overall network bandwidth efficiency.

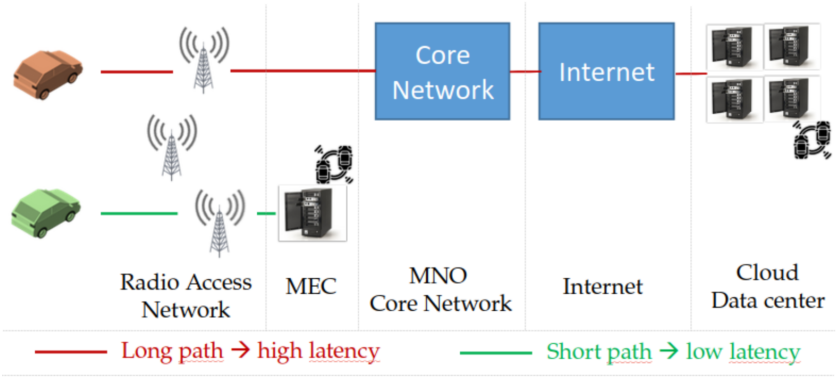

Figure 2.1: Scheme illustrating the Multi-Access Edge Computing (MEC) paradigm, using a cellular network as a reference along with a centralized collision avoidance service (depicted by the black icon with two vehicles). The red vehicle experiences significantly higher latency compared to the green vehicle, which utilizes the same service deployed on a MEC server at the network edge. From [3].

For the development of V2X wireless communication technologies, significant emphasis has been placed, since the beginning of this century, on allocating dedicated spectrum for Intelligent Transportation Systems (ITS). In 1999, the US Federal Communications Commission (FCC) allocated 75 MHz of spectrum in the 5.9 GHz band to Dedicated Short-Range Communications (DSRC). This allocation spans from 5.850 to 5.925 GHz and includes seven 10 MHz channels, together with a 5 MHz guard band between 5.850 and 5.855 GHz. The guard band was introduced to mitigate interference with adjacent services, including effects related to Doppler shifts. The IEEE also defines a standardized channel numbering scheme according to the following expression:

$$f(\mathrm{CH}) = 5000 + 5 \cdot \mathrm{CH}\,[\mathrm{MHz}] \tag{2.1}$$

where CH denotes the channel number as shown in Figure 2.2. Within this framework, the IEEE specifies one Control Channel (CCH, channel 178), which serves as the default channel for high-priority safety and control information, and six Service Channels (SCH) for additional applications. Despite strong opposition from the automotive industry and ITS stakeholders, in November 2020 the FCC unanimously adopted a First Report and Order reallocating a substantial portion of the 5.9 GHz

band. Specifically, the lower 45 MHz (5850–5895 MHz) were reassigned to unlicensed uses, such as Wi-Fi. Consequently, only the upper 30 MHz (5895–5925 MHz) remain designated for intelligent transportation systems [10].

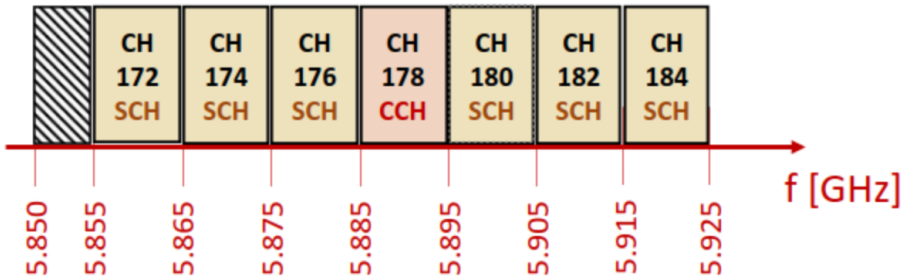

Figure 2.2: US band for V2X, from [3].

In contrast, the European Commission, through Commission Decision 2008/671/EC, designated the 5875–5905 MHz band for ITS applications within the European Union. Harmonization within the European Conference of Postal and Telecommunications Administrations (CEPT) was achieved through a decision of the Electronic Communications Committee (ECC), which further identified the 5905–5925 MHz band as a potential extension of the ITS spectrum. The current European spectrum allocation follows the technical recommendations of TR 102 492-1. In particular, 5855–5875 MHz is assigned to non-safety-related applications, 5875–5885 MHz to road-safety and traffic-efficiency services, and 5885–5905 MHz to critical road-safety applications. The control channel is located at 5.90 GHz (channel 180), while channels 182 and 184 are reserved for future use [11].

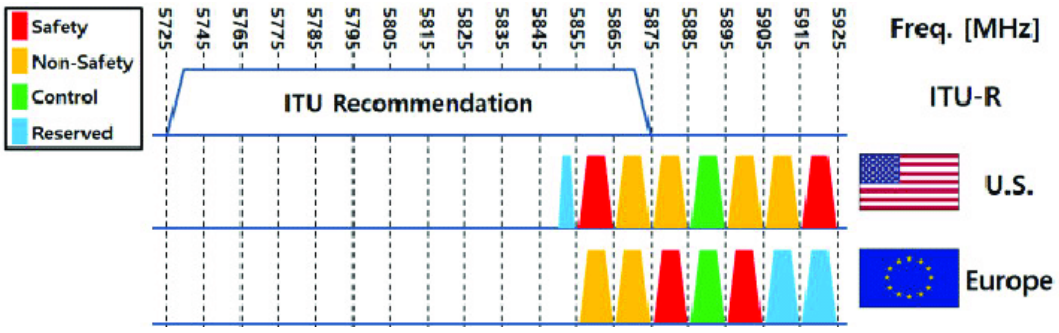

Figure 2.3: Channel division scheme for the 5.9 GHz band in Europe and the U.S.

Although the European regulatory approach is largely technology-neutral, it strongly opposes the FCC's decision to segment the spectrum and does not support sharing the ITS band with other technologies such as Wi-Fi [11]. While C-V2X is widely regarded as a promising alternative, the debate regarding the superiority of IEEE 802.11p (DSRC-based) and C-V2X remains open. Several studies in the literature analyze the respective strengths and limitations of both technologies. In general, IEEE 802.11p, being a more mature and extensively validated technology,

typically provides lower latency and better performance for aperiodic messages with variable payload sizes. Conversely, C-V2X offers improved robustness in terms of communication range and resilience to channel congestion [12], [13], [14]. The European automotive market is still awaiting further evolution and standardization of V2X technologies to identify the most suitable solution for vehicular requirements. At present, many considerations remain partly theoretical, as only a limited number of vehicles are equipped with V2X capabilities, such as the Volkswagen Golf 8 featuring a DSRC module. In Europe, spectrum regulations are technology-neutral, meaning that no specific technology is granted preferential access. Both DSRC and C-V2X are permitted to operate within the 5.9 GHz band (5855–5925 MHz). However, coexistence remains a significant challenge, as the two technologies may interfere with each other when operating on the same channel due to differences in their physical-layer protocols. The objective is therefore to define a practical and mutually compatible framework that enables both technologies to operate within the 5.9 GHz band without compromising road-safety services. A possible spectrum-sharing strategy can be structured as a gradual three-step approach [15]:

- **Step 1 – Sharing via preferred channels:** Each technology is assigned a preferred 10 MHz channel (e.g., 5875–5885 MHz for Technology A and 5895–5905 MHz for Technology B). This configuration prevents same-channel interference without requiring advanced coexistence mechanisms.
- **Step 2 – Preferred channels with detect-and-vacate on the central channel (5885–5895 MHz):** A detect-and-vacate mechanism is introduced. A technology may transmit on the shared central channel only if it does not detect transmissions from the other technology on that channel.
- **Step 3 – Extended detect-and-vacate on adjacent channels:** The detect-and-vacate mechanism is further extended not only to the central shared channel but also to the channels primarily assigned to the other technology.

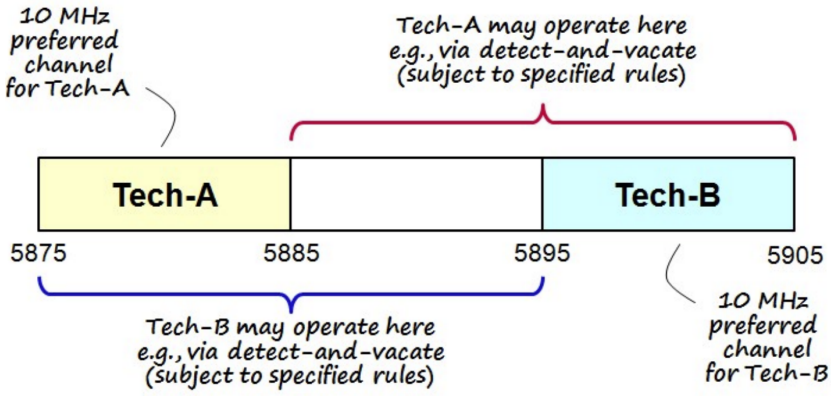

Figure 2.4: Step-3: Sharing of 5.9 GHz, via preferred channels complemented by mutual detect-and vacate extended to the lower and upper 10 MHz channels, from [15].

Once coexistence mechanisms have sufficiently matured, full sharing of the entire 5855–5925 MHz band may become feasible.

A further step toward effective coexistence is represented by the new Qualcomm V2X 350 chipset, which supports all major V2X radio technologies, including DSRC and C-V2X. The chipset is capable of operating two radios simultaneously, each equipped with dual antennas and full transmit/receive diversity. Although this solution has not yet been widely integrated into commercial vehicles, such multi-radio architectures, combined with dedicated channel-switching algorithms, are expected to enable high performance in future coexistence scenarios [16].

2.1 DSRC-based protocols

Dedicated Short-Range Communications (DSRC) is a Wi-Fi-based communication technology specifically designed for vehicular environments. Its communication stack relies on IEEE 802.11p and the more recent IEEE 802.11bd standards at the Physical (PHY) and Medium Access Control (MAC) layers, while the upper layers are defined by the IEEE 1609.x family of standards.

2.1.1 IEEE 802.11p

IEEE 802.11p is a specific amendment to the IEEE 802.11 standard, published in 2010, several years after the FCC's allocation of the 5.9 GHz band. It is now incorporated into the IEEE 802.11-2024 family of standards [17]. IEEE 802.11p is one of the most widely adopted DSRC standards for V2X communications and is based on the IEEE 802.11a amendment. Unlike IEEE 802.11a, which operates at 5 GHz, IEEE 802.11p operates in the 5.9 GHz band. It employs Orthogonal Frequency-Division Multiplexing (OFDM) with a "half clock" configuration, reducing the channel bandwidth from 20 MHz to 10 MHz [18]. The system is based on 64 orthogonal subcarriers and supports data rates ranging from 3 Mb/s to 27 Mb/s, depending on the selected Modulation and Coding Scheme (MCS). The supported modulation schemes include BPSK, QPSK, 16-QAM, and 64-QAM. As a consequence of the reduced channel bandwidth, the timing parameters are doubled, and the OFDM symbol duration becomes 8 μs [19], as shown in table2.1.

Parameter	**IEEE 802.11a**	**IEEE 802.11p**
Sample rate	20 MHz	10 MHz
Modulation scheme	BPSK, QPSK, 16QAM, 64QAM	BPSK, QPSK, 16QAM, 64QAM
Coding scheme	1/2	1/2
Puncturing	optional puncturing 3/4 or 2/3	3/4 or 2/3
Available data rate	6, 9, 12, 18, 24, 36, 48, 54 Mbps	3, 4.5, 6, 9, 12, 18, 24, 27 Mbps

Table 2.1: Comparison between IEEE 802.11a and IEEE 802.11p [19]

Although this approach leads to a reduction in throughput, it significantly improves robustness against Doppler effects, fading, and multipath propagation, as

well as inter-symbol interference (ISI) and inter-carrier interference (ICI). At the MAC layer, IEEE 802.11p is based on CSMA/CA, with Quality of Service enhancements derived from IEEE 802.11e. Two main characteristics are specific to IEEE 802.11p:

- The Outside the Context of a Basic Service Set (OCB) mode is a specific operating mode introduced to eliminate the latency associated with establishing a Basic Service Set (BSS). In particular, it removes the need for the conventional IEEE 802.11 authentication and association procedures.Under standard IEEE 802.11 operation, each compliant station must include in the MAC header a 48-bit BSSID value identifying the BSS to which it belongs. In OCB mode, however, a station transmits frames only when the dot11OCBActivated flag is set to true. In this case, the transmitting station sets the BSSID field to the wildcard BSSID value, indicating that it is not associated with any BSS. When operating in OCB mode, the station is not part of a BSS and therefore does not make use of IEEE 802.11 authentication, association, or data confidentiality services. Any required authentication mechanisms are instead handled by the Station Management Entity (SME), which is also responsible for determining the PHY parameters, such as the transmission channel, and managing any changes to the operating channel.[17]

- The use of the so-called Enhanced Distributed Channel Access (EDCA), a priority-based access method built on four Access Categories (ACs), derived from eight User Priorities (UPs):

  - **AC_BK**(Background): the lowest priority, corresponds to UPs 1 and 2
  - **AC_BE**(Best Effort): corresponds to UPs 0 and 3
  - **AC_VI**(Video): corresponds to UPs 4 and 5
  - **AC_VO**(Voice): corresponds to UPs 6 and 7

  Each Access Category corresponds to a specific queue within the MAC layer. An internal contention algorithm independently calculates the backoff for each queue based on the access parameters. The queues perform internal contention among themselves: the "winning" queue is the one with the smallest backoff time, while the others continue their backoff procedure. Instead of the Distributed Coordination Function Interframe Space (DIFS), this channel access method defines four Arbitration Interframe Spaces (AIFS), whose durations depend on the priority of the traffic:

  $$\text{AIFS}(AC) = \text{AIFSN}(AC) \cdot SlotTime + SIFS$$

  In this way, shorter AIFS values, corresponding to higher-priority traffic, probabilistically result in lower waiting times. Furthermore, the backoff procedure depends on the Contention Window (CW), whose value increases between CWmin and CWmax each time a collision occurs [20].

Access Category	CWmin	CWmax	AIFSN	AIFS [μs]
AC_BK	15	1023	9	149
AC_BE	15	1023	6	110
AC_VI	7	15	3	71
AC_VO	3	7	2	58

Table 2.2: According to IEEE 802.11-2024, AIFS and contention window sizes for each AC, with a Slottime=13 µs, while the SIFS time is 32 µs [17]

2.1.2 IEEE 802.11bd

However, although IEEE 802.11p is a well-established technology, it is still based on earlier amendments such as IEEE 802.11a and IEEE 802.11e. For this reason, IEEE has undertaken efforts to define a new standard specifically tailored to vehicular communications. The IEEE 802.11bd standard represents the most recent evolution of Vehicle-to-Everything (V2X) communications and has been designed to meet the increasingly stringent requirements of intelligent transportation systems and autonomous driving. It was conceived as a direct enhancement of IEEE 802.11p, addressing the limitations that have emerged over time in terms of throughput, reliability, robustness, and coverage, and defining both the PHY and MAC layers. Emerging applications such as collective perception, cooperative maneuvers, hazard warning messages, event-driven messaging, and especially Cooperative Automated Driving (CAD) demand performance levels that IEEE 802.11p cannot guarantee. Indeed, IEEE 802.11p exhibits structural limitations in coverage, transmission capacity, and flexibility. Issues such as low signal quality, inefficient radio resource allocation, limited capability in handling Doppler effects, and insufficient Modulation and Coding Schemes [21]. IEEE 802.11bd introduces significant innovations at both the PHY and MAC layers, while ensuring coexistence with IEEE 802.11p. Some physical improvements are:

- In IEEE 802.11p, the standard operates exclusively in the 5.9 GHz band with 10 MHz channels. IEEE 802.11bd introduces significant improvements in frequency allocation, expanding and making spectrum usage more flexible. It also includes support for unlicensed frequencies in the mmWave band, in addition to supporting both 10 MHz and 20 MHz channels with a dynamic channel switching mechanism, adapting to application requirements and traffic conditions. Each 10 MHz channel comprises 64 Orthogonal Frequency Division Multiplexing subcarriers, with 52 dedicated to data transmission, whereas a 20 MHz channel uses 128 subcarriers, of which 108 are allocated for data.

- In addition to the frame preamble, midambles, inserted into the data field with a periodicity of 4, 8, or 16 OFDM symbols, play a pivotal role in obtaining up-to-date channel estimation information. They provide improved channel estimation accuracy and reduce the packet error rate (PER).

- It introduces new Modulation and Coding Schemes, featuring higher-order

modulations and a consequent increase in data rate. The "bd" amendment supports modulation schemes up to 256-QAM and coding rates up to 5/6, achieving data rates of up to 90 Mbps, whereas IEEE 802.11p is limited to 27 Mbps with 64-QAM modulation and a 3/4 coding rate. urthermore, it introduces Dual Carrier Modulation (DCM), a technique inherited from IEEE 802.11ax, which allows stations to modulate and transmit each data symbol over two subcarriers. This approach improves reception probability and enhances robustness against interference and fading, particularly in weak signal conditions, extending the communication range by up to three times. With higher MCS levels, Forward Error Correction (FEC) plays a crucial role. The standard adopts LDPC coding, which significantly enhances error correction capabilities. In combination with midambles, and under high SNR conditions, this enables data rates nearly three times higher than those achievable with the previous standard [21].

Several improvements are also introduced at the MAC layer. These include the possibility of retransmitting the same broadcast message up to three times, separated only by a Short Interframe Space (SIFS). A new parameter, referred to as "fallback enabled," is introduced: when a 20 MHz channel is occupied, it enables transmission over a 10 MHz channel. In addition, block aggregation is permitted—unlike in IEEE 802.11p, but only for unicast transmissions. The introduction of 20 MHz channels and the fallback-enabled mechanism has required corresponding enhancements to the EDCA method.

2.1.3 WAVE

In the United States, the IEEE WAVE (Wireless Access in Vehicular Environments) protocol suite is composed of the IEEE 1609.x family of standards [22]. It is built upon IEEE 802.11p for the PHY and MAC layers, and IEEE 802.2 for the Logical Link Control (LLC) layer. Together, these standards form the so-called WAVE stack, specifically designed for the U.S. market and optimized for vehicular communications. The main standards in the IEEE 1609 family include IEEE P1609.1, which defines management activities; IEEE P1609.2, which specifies security protocols; and IEEE P1609.3, which defines the network-layer protocol. Above the PHY and MAC layers, IEEE 1609.4 defines multi-channel operation, including channel coordination, channel routing, and time synchronization. These functions are specified as part of an "upper" MAC layer, extending the IEEE 802.11p MAC. The Control Channel is the default channel used for WAVE Service Advertisements (WSAs) and management messages, while application-related data are transmitted over the SCHs. In addition, the standard defines a channel switching mechanism to efficiently alternate between the CCH and SCHs [23].

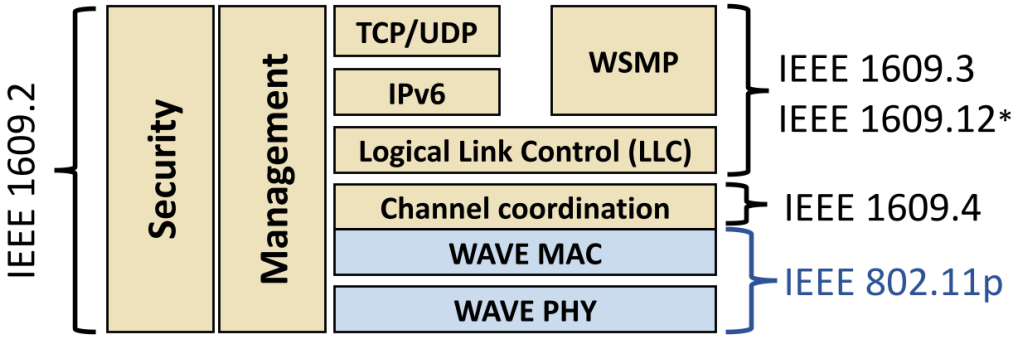

Figure 2.5: The IEEE WAVE, from [3]

The Application, Presentation, and Session layers of the ISO/OSI model are not explicitly defined within the WAVE standards. Instead, these layers are specified by SAE. In particular, the SAE J2735 standard defines a set of message types, ranging from safety-critical periodic messages to more application-oriented communications [24].

2.2 C-V2X

In recent years, attention has increasingly shifted toward another communication paradigm: Cellular Vehicle-to-Everything (C-V2X), a cellular-based network technology specifically designed for VANET applications. C-V2X has been standardized since 3GPP Release 14. The 3GPP focuses on integrating V2X communications into cellular networks and therefore specifies mainly the lower layers of the protocol stack, namely the PHY and data link layers. C-V2X appears promising in several respects, including greater resilience to channel congestion, the ability to use both the Uu interface for network-based communication and the PC5 interface for direct V2V data exchange, as well as broader radio coverage compared to IEEE 802.11p. Furthermore, the 5.9 GHz Second Report and Order issued by the FCC designated C-V2X as a technology for the U.S. ITS band [25]. The development of C-V2X began with 3GPP Release 12, which introduced Device-to-Device (D2D) communication under the ProSe (Proximity Services) framework, initially intended for public safety applications and later extended to other use cases. The first fully defined C-V2X standard, known as LTE-V2X, was introduced in Release 14 and was based on Long Term Evolution (LTE) and D2D communication. The most recent evolution is NR-V2X, introduced in 3GPP Release 16 and based on 5G New Radio (NR). Although the Radio Access Technology (RAT) used in LTE-V2X differs significantly

from the previously defined DSRC technology, the protocol layers above the radio interface remain largely aligned between C-V2X and DSRC.

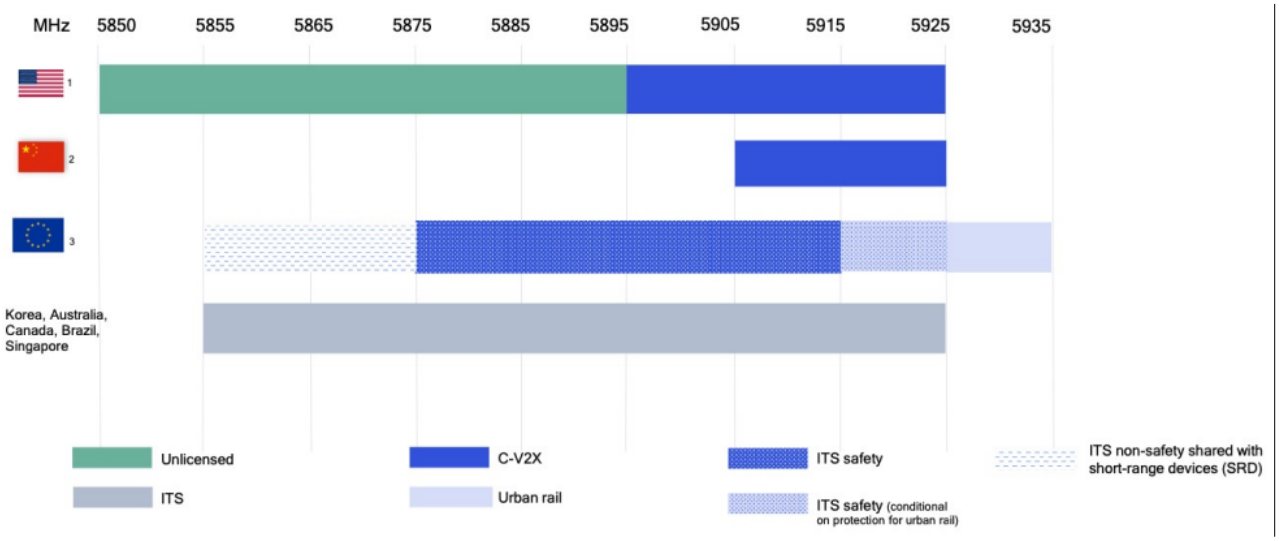

Figure 2.6: 5.9 GHz band frequency utilization

2.2.1 LTE-V2X

LTE-V2X implements two types of interfaces:

- The *PC5* sidelink interface, used for V2V, V2P, and V2I communications. This interface enables different User Equipments (UEs), representing VANET nodes, to communicate directly over the 5.9 GHz band, similarly to DSRC.
- The *Uu* interface is used for V2N communication towards a base staion (eNodeb). It enables communication over the licensed spectrum through standard uplink and downlink transmissions.

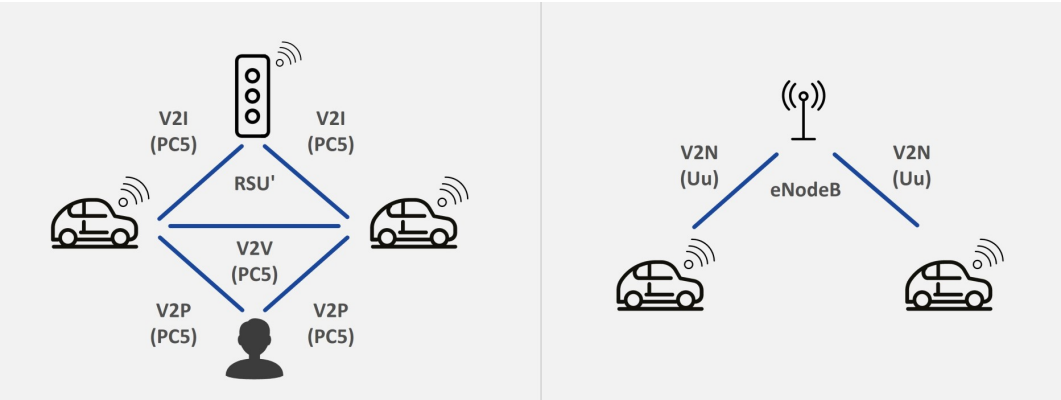

Figure 2.7: C-V2X Communication Modes

V2X communication over the sidelink is supported in two modes: *(i)* when the UE is within LTE network coverage (Mode 3), where the infrastructure manages the D2D communication, including resource selection and configuration; and *(ii)* when

the UE is outside network coverage (Mode 4), where vehicles autonomously select and configure the resources and subchannels. Mode 4 does not require a SIM card or an operator subscription.

Mode 3 can provide superior performance compared to Mode 4, as resources are centrally managed; however, it requires the node to remain under network coverage [26]. Mode 4, on the other hand, is generally preferred for safety-related communications because it can operate without cellular infrastructure [27]. The physical layer of LTE-V2X employs the SC-FDMA (Single-Carrier Frequency Division Multiple Access) technique and supports channel bandwidths of 10 MHz and 20 MHz. The available bandwidth is divided into Resource Blocks (RBs) of 180 kHz, each composed of 12 subcarriers spaced by 15 kHz. In the time domain, the channel is structured into subframes, each with a duration of 1 ms and consisting of 14 OFDM symbols. Of these, nine symbols are allocated for data transmission, four are reserved for specific functions such as channel estimation and Doppler mitigation, and one serves as a guard symbol for timing adjustments. Resource Blocks are grouped into subchannels, each containing only RBs belonging to the same subframe. The number of RBs per subchannel is preconfigured and may vary. Data are organized into Transport Blocks, each carrying a complete packet and potentially occupying multiple subchannels depending on the configuration. Each TB is associated with Sidelink Control Information (SCI), without which the TB cannot be decoded. The SCI occupies two RBs and includes information such as the RBs allocated to the corresponding TB, the Modulation and Coding Scheme, the priority of the transmitted message, whether the transmission is an initial transmission or a blind retransmission, and the resource reservation interval. A blind retransmission refers to a scheduled retransmission or repetition of a TB that is not based on receiver feedback. The resource reservation interval specifies when the vehicle will use the reserved subchannel(s) to transmit the next TB. In the frequency domain, two main channels are defined: the Physical Sidelink Shared Channel (PSSCH), which carries the Transport Blocks (TBs), and the Physical Sidelink Control Channel (PSCCH), which carries the Sidelink Control Information (SCI). As previously mentioned, these channels may be allocated either adjacently or non-adjacently [26].

LTE-V2X does not define a specific algorithm for subchannel selection in Mode 3; instead, it specifies two scheduling approaches: dynamic scheduling and Semi-Persistent Scheduling (SPS). In dynamic scheduling, vehicles request subchannels from the eNB for each Transport Block (TB). In SPS, the eNB reserves subchannels that enable a vehicle to transmit multiple TBs, with the periodicity of the reserved resources configurable by the eNB. However, Mode 3 requires operation under network coverage and introduces additional uplink (UL) and downlink (DL) signaling overhead. To address scenarios in which neighboring vehicles are served by different operators, 3GPP has defined a specific architectural framework [26]. In Mode 4, vehicles autonomously select subchannels using sensing-based Semi-Persistent Scheduling. A vehicle announces the reservation of the selected subchannels for the transmission of the next TB by including the Resource Reservation Interval (RRI) in the SCI.

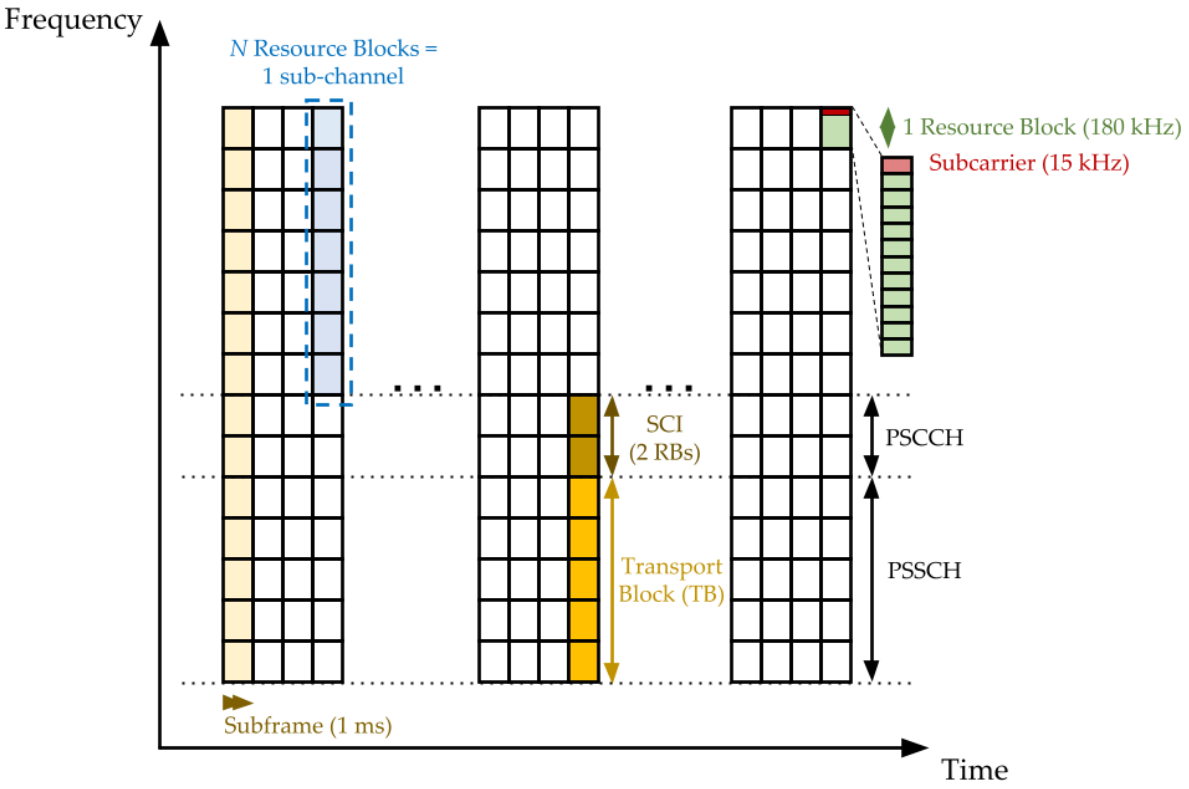

Figure 2.8: Time-frequency division of LTE-V2X channels, with adjacent Physical Sidelink Shared Channel and Physical Sidelink Control Channel, from [3].

The RRI may be set to 0 ms, 20 ms, 50 ms, 100 ms, or any multiple of 100 ms up to a maximum of 1000 ms. Only RRI values greater than 0 ms can be selected from a preconfigured list of permitted values; the value 0 indicates that the vehicle is not reserving the same subchannel. The Reselection Counter (RC) is randomly chosen within a range that depends on the selected RRI. It is decremented at each transmission, and when it reaches zero, the vehicle reselects resources with probability $1 - P$, where $P \in [0, 0.8]$ and depends on the environment. Resource reselection may also occur if the data frame exceeds the allocated resources or if the selected RRI is greater than the message period. When a vehicle needs to select new subchannels through SPS, it first identifies a set of candidate resources within a Selection Window (SW). It then excludes resources deemed unsuitable based on sensing information collected over the previous 1000 subframes. The remaining resources form list L1. If the ratio between candidate resources and the total number of resources falls below 20%, the power threshold is increased by 3 dB. From L1, the vehicle selects a subset characterized by the lowest average Received Signal Strength Indicator (RSSI), forming list L2. Finally, one resource is randomly chosen from L2 to reduce the probability of collisions. This resource is assigned for transmission of the new TB until the RC expires [26].

2.2.2 NR-V2X

LTE-V2X was introduced in 3GPP Releases 14 and 15 with the primary objective of supporting basic V2X safety applications. In contrast, 5G-V2X, defined starting from Release 16, was designed to enable advanced use cases such as cooperative driving and coordinated maneuvers. Consequently, 5G-V2X adopts several differences, including:

- Mode 3 and Mode 4 are respectively replaced by Mode 1 and Mode 2, with Mode 2 representing the new infrastructure-less communication mode.
- Unlike LTE-V2X, which supported only periodic messages, 5G-V2X considers both periodic and aperiodic traffic from the outset of its specifications [28].
- For NR sidelink (SL) in Release 16, two frequency bands are defined for the PC5 interface: the 5.9 GHz band and the 2.5 GHz band. However, only the 5.9 GHz band is reserved for ITS purposes.
- NR-V2X now supports unicast and groupcast transmissions, in addition to broadcast communications [29].
- In LTE-V2X, sidelink communication supports only a subcarrier spacing of 15 kHz, resulting in a fixed subframe duration of 1 ms. In Release 16, multiple subcarrier spacings are supported, defined as $\Delta f = 15 \cdot 2^{\mu}\,\text{kHz}, \quad \mu \in \{0, 1, 2, 3\}$. Therefore, the possible subcarrier spacings are 15, 30, 60, and 120 kHz. The slot duration is variable and depends on the selected subcarrier spacing, being equal to $2^{-\mu}$ ms.
- n LTE-V2X, during sensing-based resource identification, the UE ensures that the ratio between the number of identified candidate resources and the total number of available resources is greater than 20%. In the updated specification, this threshold is configurable and may take values of 20%, 35%, or 50%, depending on the priority level of the sidelink transmission, as defined by the standard.
- In contrast to LTE-V2X, NR-V2X defines a pre-emption check mechanism, which allows previously reserved resources to be released if specific conditions are met.
- In LTE-V2X, once resources are selected, no further verification is specified before the actual transmission. In NR-V2X, a re-evaluation check is introduced: the UE performs additional sensing prior to transmission to verify whether the pre-selected resources are still included in the identified resource set. If the resources are no longer valid, a resource reselection procedure is triggered.
- With Release 17, NR-V2X introduces energy-efficient resource allocation mechanisms, including partial sensing and random resource selection. NR-V2X partial sensing can be implemented through two approaches: periodic-based partial sensing (PBPS) and contiguous partial sensing (CPS). In PBPS, the

UE does not perform continuous sensing; instead, it monitors a limited set of sensing occasions that are periodically spaced according to the reservation periodicities supported by the resource pool. In CPS, sensing is restricted to a single contiguous sensing window with a defined start and end, representing a subset of the resource selection window.

The improvements introduced by NR-V2X can provide up to a 20% increase in reliability compared to LTE-V2X. Moreover, the NR-V2X partial sensing scheme can achieve up to a 95% reduction in power consumption compared to the full sensing scheme [30].

2.3 C-ITS

While IEEE standards dominate the landscape in North America, ETSI defines the Cooperative Intelligent Transport Systems (C-ITS) standards for Europe. Although primarily developed for the European context, these standards can be adopted worldwide, particularly with regard to the standardized C-ITS messages. Since 2007, drawing inspiration from the WAVE architecture, ETSI has developed the ITS-G5 protocol stack. For ITS access technologies, ETSI adopts IEEE 802.11p as the baseline standard, as described in [31]. In addition to reusing these standards, ITS-G5 introduces mechanisms for Decentralized Congestion Control (DCC). DCC methods regulate channel load dynamically in order to prevent network congestion and avoid unstable system behavior, which is particularly important in high-density vehicular scenarios. The two lowest layers of the ITS communication stack are referred to as the Access Layer, and the technologies specified for this layer are collectively known as ITS-G5. ITS-G5 is based largely on already existing IEEE standards for wireless communication. Within the Access Layer, the Data Link Layer is divided into two sublayers: medium access control and logical link control. Originally, the Physical layer and the MAC layer were defined in IEEE 802.11p, which was specifically designed for vehicular environments. The LLC sublayer is based on ANSI/IEEE Std 802.2. In addition to reusing these standards, ITS-G5 introduces mechanisms for Decentralized Congestion Control. DCC methods regulate channel load dynamically in order to prevent network congestion and avoid unstable system behavior, which is particularly important in high-density vehicular scenarios. so we can refer to ITS-G5 as an access technology based on DSRC plus some congestion control feature. So we can refer to ITS-G5 as an access technology based on DSRC plus some congestion control feature. In more recent years, ETSI has also made efforts to integrate new access technologies, such as LTE-V2X, into the stack, providing guidelines for their interconnection with higher layers, as outlined in [32].

The C-ITS protocol stack for a connected vehicle is illustrated in Figure4.4. It organizes the ISO/OSI network model into four layers. Unlike WAVE, ITS-G5 also standardizes the upper layers of the ISO/OSI model, specifically the Session, Presentation, and Application layers.

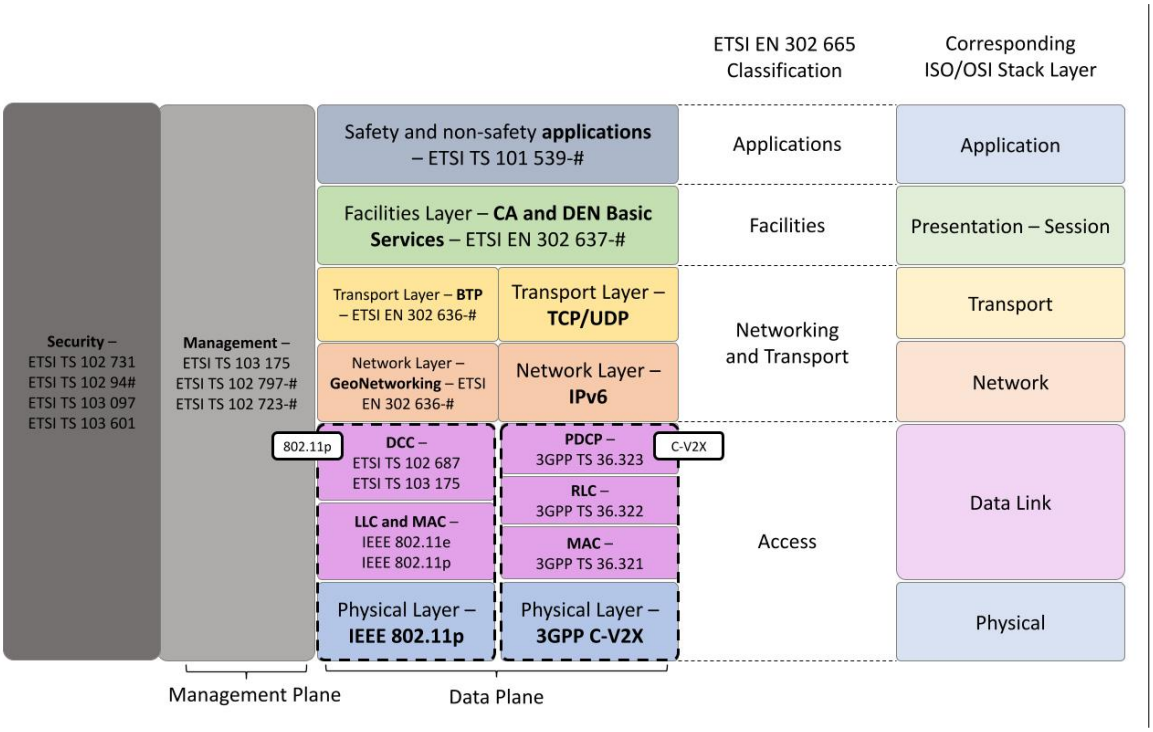

Figure 2.9: Standardized network stack for a connected vehicle as defined by ETSI. Each layer corresponds to a specific OSI/ISO layer, and the relevant standards (ETSI, IEEE, and 3GPP) are reported below, from [3].

Applications layer

The application layer is responsible for implementing cooperative and safety ITS applications, which rely on the exchange of standardized messages between VANET nodes.

Facilities layer

Moving down the stack, the Facilities layer is found, playing a pivotal role in the ETSI architecture, and it is organized into three sub-layers:

- Information Support Layer: provides facilities that support the collection and management of data, such as the Local Dynamic Map (LDM).
- Communication Support Layer: provides services for communication and session management.
- Application Support Layer: provides application-level functionalities for the ITS Basic Set of Applications (ITS BSA), including the encoding and decoding of a set of standardized messages.

Similar to SAE J2735, the ETSI C-ITS protocol suite defines several standardized message types. The most relevant ones are described below:

- **Cooperative Awareness Message (CAM):** it is a periodic message storing information about position, heading, speed acceleration and other informa-

tion on state of the vehicles. The CA basic service It provides two main services:sending and receiving of CAMs. The default transmission rate is set at 1 Hz but if any of this three situation occour the frequency is set at 10 Hz: (i) there is a speed variation of 4 m/s, (ii) the difference between the current heading and the last CAM heading is up to 4° and (iii) the position variation exceeds 4 m. [33]

- **Decentralized Environmental Notification Messages (DENM):** The transmission and reception of DENMs are managed by the so-called Decentralized Environmental Notification Basic Service (DEN Basic Service), located in the Facilities Layer. A DENM is an event-based broadcast message that conveys information about the event that triggered its generation. DENMs have a local scope and are routed within a specific geographical area. [34]

- **Infrastructure to Vehicle Information Message (IVIM):** The IVI service manages the generation, transmission, and reception of IVIM messages. These messages are used in I2V communications to support mandatory and advisory road signage information.[35].

- **Services Announcement Essential Message (SAEM):** This message acts as a service announcement and provides information about the ITS services that are available [36].

- **MAP (topology) Extended Message (MAPEM) and Signal Phase And Timing Extended Message (SPATEM):** These messages carry information about the current road topology and, respectively, real-time data on the signal phase and timing of traffic lights at an intersection. [35].

- **Vulnerable Road Users Awareness Message (VAM):** The VRU Awareness Basic Service enables the transmission and reception of VAM messages. These messages serve safety-related purposes, such as pedestrian collision avoidance. VAMs operate similarly to CAMs but are transmitted by Vulnerable Road Users (VRUs). The message generation frequency is determined based on changes in kinematic parameters and may vary between 0.2 Hz and 10 Hz, depending on the VRU's state and location. VRUs may also form a single entity, referred to as a cluster. In this case, only the cluster leader transmits messages, which also describe the overall state of the cluster. [37]

- **Cooperative Perception Message (CPM):** The Collective Perception Service enables vehicles and other ITS stations to exchange information about what they "perceive" in their surrounding environment through Collective Perception Messages (CPMs). These messages support collective perception by conveying information about objects detected via on-board sensors, such as cameras and radars. The shared data enhances situational awareness of both connected and non-connected objects. CPMs are expected to include a list of

detected objects, along with their positions and relevant information about the sensing capabilities used for detection. [38]

Each message includes a mandatory part containing: *(i)* the station ID, which identifies the transmitting ITS entity; *(ii)* the protocol version, which specifies the version of the message (for example, two versions of CAM are currently defined); and *(iii)* the message ID, which identifies the type of message.

All messages standardized within the ETSI Facilities Layer are defined using Abstract Syntax Notation One (ASN.1). "ASN.1 is a formal notation used for describing data transmitted by telecommunications protocols" [39], enabling the definition of complex data types in a platform-independent way. An ASN.1 module starts with the module name, followed by the keywords DEFINITIONS AUTOMATIC TAGS ::= and BEGIN. Inside the module, items are declared together with their respective types. The module is terminated by the keyword END. For example:

```
ModuleName DEFINITIONS AUTOMATIC TAGS ::=
BEGIN
ItemName1 ::= ItemType1
ItemName2 ::= ItemType2
END
```

After defining the content of a message using ASN.1, several encoding rules are available to specify how the message is encoded and decoded. All ETSI standard-compliant messages, such as IVIMs, make use of UPER (Unaligned Packed Encoding Rules), which ensures compact message sizes [35].

Networking and Transport layer

The ITS Networking and Transport Layer comprises protocols for data delivery among ITS stations and from ITS stations to other network nodes. With regard to the transport protocol, ITS-G5 defines the Basic Transport Protocol (BTP), specified by ETSI in [31] for ITS-G5. Similar to UDP, BTP provides an end-to-end, connectionless transport service for ITS ad hoc networks. The purpose of this protocol is to enable the ITS Facilities Layer to access the services of the GeoNetworking protocol. To facilitate this mechanism, BTP uses ports: each port represents a communication endpoint that identifies the ITS Facilities Layer service at the source or destination. Communication between BTP and the Facilities Layer occurs through the BTP Service Access Point (BTP-SAP), which adds a minimal header to identify the destination service and encapsulates the control information together with the payload into a BTP-PDU, which is then forwarded to GeoNetworking [31]. The BTP header is 4 bytes long. ETSI defines two types of packets: (i) BTP-A, for interactive communication sessions, which contains both a destination port and a source port; and (ii) BTP-B, for non-interactive communication sessions, which carries only the destination port. In this case, the source port field is replaced by destination port information, which is normally unused and set to 0 by default. The standard also

assigns a BTP port number to each vehicular message type [40]. BTP port numbers and message IDs are summarized in Table2.3.

Message	Message ID	BTP port number
CAM	2	2001
DENM	1	2002
IVIM	6	2006
MAPEM	5	2003
SPATEM	4	2004
VAM	14	2018

Table 2.3: message IDs and BTP port number for the most common ETSI C-ITS messages.

GeoNetworking (GN) is a network-layer ad hoc protocol for VANETs, characterized by the use of geographical positioning for information dissemination. Each ITS station has two main roles: first, it acts as a network node and can operate as a communication source or sink; likewise, it may forward data. Second, it can operate at the network edge and interconnect different networks via an ITS station internal network [41]. The geographical addressing and forwarding capabilities provided by GN allow the definition of a set of communication scenarios. The set of communication scenarios defined in [42], which GN is designed to support, includes:

- Point-to-Point: Communication starts at a single ITS station and terminates at a single ITS station. This scenario is supported by the GeoUnicast forwarding scheme defined in GeoNetworking.In this scheme, when a node transmits a unicast packet, it first determines the geographical position of the destination node. The packet is then forwarded to a neighboring node located in the direction of the destination. Each intermediate node subsequently re-forwards the packet along the path, until it finally reaches the intended destination. [43].

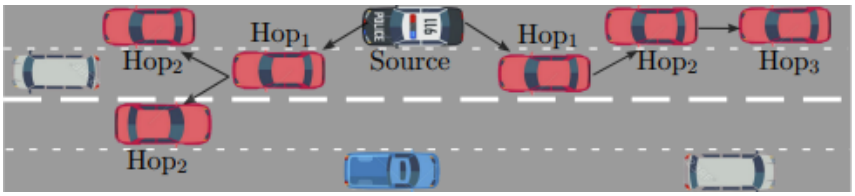

Figure 2.10: GeoUnicast, from [44]

- Point-to-Multipoint: Communication originates from a single ITS station and is intended for multiple ITS stations. This scenario is described by the Topologically-Scoped Broadcast (TSB) forwarding scheme defined in GN, in which ITS stations rebroadcast a data packet from a source to all nodes within the n-hop neighborhood inside the communication range [43]. specific case of TSB, used for transmitting a CAM message, is referred to as Single Hop Topologically-Scoped Broadcast. In this case, the message is disseminated only to the immediate first-hop neighbors, and no further forwarding is required.

This forwarding scheme is also used by IVIM messages when the dissemination area is within the direct communication range of the sending ITS station.

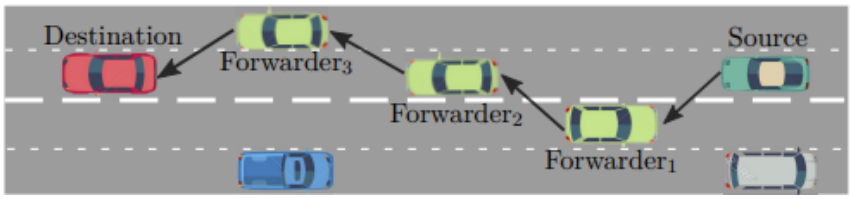

Figure 2.11: Topologically-scoped broadcast, from [44]

- GeoAnycast: Communication originates from a single ITS station and is directed to an arbitrary vehicle ITS station located within a specific geographical area. In this scenario, packets are forwarded on a hop-by-hop basis until they reach the destination area specified in the packet.

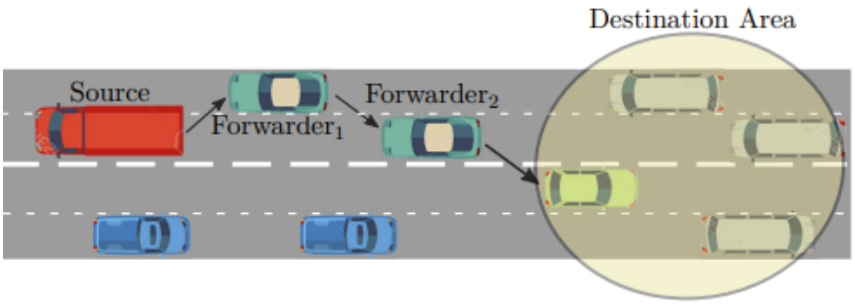

Figure 2.12: GeoAnycast, from [44]

- GeoBroadcast: Communication originates from a single vehicle ITS station and is intended for multiple vehicle ITS stations within a specified geographical area. This scenario uses the same forwarding scheme as GeoAnycast, with the difference that once the packet reaches a node inside the destination area, all nodes within that area rebroadcast the packet. This forwarding scheme is used for ITS DEN service messages and for IVIM messages when the dissemination area extends beyond the direct communication range of the infrastructure.

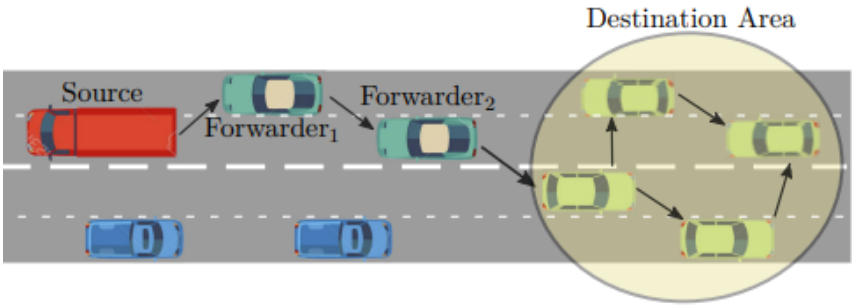

Figure 2.13: GeoBroadcast, from [44]

Access layer

As introduced at the beginning of this section, for ITS access technologies ETSI

adopts DSRC and C-V2X as the baseline standards for the MAC and Physical layers. On top of the access layer, ITS-G5 defines one of its key mechanisms to address the highly dynamic nature of VANETs, namely Decentralized Congestion Control [45]. DCC operates as a state machine, where transitions among three states *Relaxed*, *Active*, and *Restrictive* are determined by the Channel Busy Ratio (CBR). The CBR is defined as the ratio of the time during which the channel is sensed as busy to the total channel sensing time. The channel is considered busy when the receiver detects a signal power exceeding a predefined threshold.

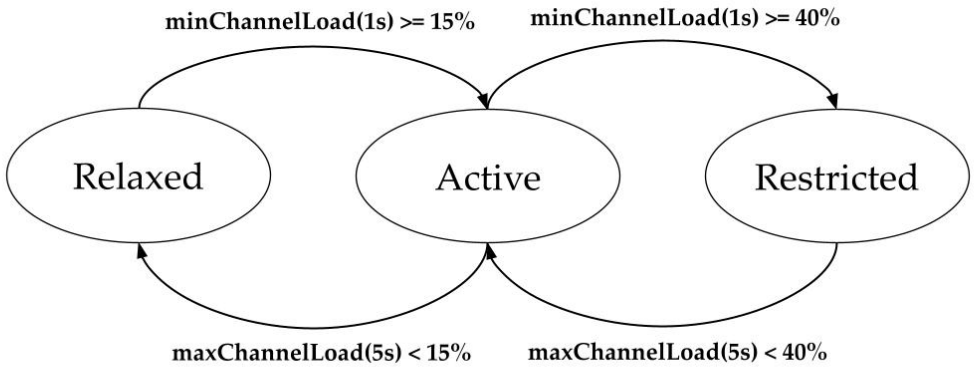

Figure 2.14: DCC state machine, from [3]

The purpose of DCC is to adapt transmission and sensing parameters according to the current network load. Each state is characterized by four configurable mechanisms, defined for each Access Category: transmission power, minimum inter-packet time, transmission data rate, and Clear Channel Assessment (CCA) sensitivity. The rightmost state, *Restrictive* which corresponds to scenarios with a high density of connected vehicles—is characterized by lower transmission power, thereby reducing interference, as well as a longer inter-packet interval and a higher modulation scheme. This results in shorter packets transmitted less frequently. Conversely, the leftmost state, corresponding to the lowest network load, increases the transmission power while reducing both the data rate and the inter-packet interval. A revised version of the DCC technical specification, released by ETSI in 2018, proposes parameter settings for a three-active-state configuration, together with a novel adaptive congestion control approach. [46]. ETSI also defines a congestion control mechanism for communication over PC5 in LTE-V2X [47], based on the ProSe Per Packet Priority (PPPP), which assigns traffic priority similarly to IEEE 802.11p through the use of Access Categories.

2.4 GNSS

The Global Navigation Satellite System (GNSS) is a fundamental technology for the development of Location-Based Services (LBS), as it provides precise, low-latency positioning essential for applications such as Automatic Vehicle Location (AVL), tracking systems, navigation, and Intelligent Transportation Systems.

Currently, GNSS consists of a constellation of 24 satellites in Earth orbit, capable of ensuring global coverage and accurate positioning. The system includes constellations developed by the United States (GPS), Russia (GLONASS), Europe (Galileo), China (BeiDou), and Japan (QZSS). The satellites operate on semi-synchronous orbits with a period of approximately 12 hours and are arranged so that at least six satellites are always visible from any point on the Earth's surface.[48]

The integration of advanced technologies has extended GNSS beyond its traditional navigation functions. A significant technological advancement is represented by Real-Time Kinematics (RTK), which enables centimeter-level accuracy through the use of carrier-phase measurements of satellite signals. The RTK system employs a fixed base station that generates correction data and transmits it to the GNSS receiver, significantly improving LBS performance in various sectors, including precision agriculture and the automotive industry.

GNSS modules transmit positioning, status, and time data through specific communication protocols, which ensure data integrity and standardization, enabling reliable and secure information exchange. Among the most widely used protocols are UBX and NMEA.

The UBX protocol, developed by u-blox for its GNSS receivers, uses a binary format instead of the text-based format typical of NMEA. This allows for greater efficiency, improved reliability through binary checksum verification, and optimized resource usage. Moreover, UBX provides broader and more flexible device control, allowing configuration parameters to be modified during operation via dedicated configuration messages (UBX-CFG).

The NMEA protocol, originally designed for marine applications, has become widely adopted in positioning systems due to its simple and lightweight ASCII format. Each NMEA sentence begins with the character "$", ends with an asterisk followed by a two-character checksum, and contains comma-separated fields. Although it offers more limited capabilities compared to binary protocols, it provides essential information in a clear and easily interpretable format.

Chapter 3

Embedded solutions for V2X

As previously discussed, the automotive industry is currently experiencing a phase of stagnation, mainly due to the lack of clear regulations regarding the standards and technologies to be adopted for vehicular communication. Europe has declared a neutral position with respect to the technology to be used, whereas the United States, following recent FCC reports, appears to be more oriented toward C-V2X, having allocated a dedicated frequency band to this technology. Therefore, in the near future, at least within Europe, it is reasonable to expect that both C-V2X and DSRC technologies will be implemented in vehicles. For this reason, an initial comparative study on the coexistence of these two technologies has been conducted within this thesis. Latency has been selected as the primary metric for this analysis, evaluated both in a free-flowing VANET scenario and in a congested network condition. In this context, latency is defined as the time elapsed between the generation of a message on one board and its effective reception on another board. This section briefly describes the hardware components adopted to implement all the software solutions and to conduct the tests required for the study.

3.1 Cohda MK6

Cohda's V2X stack and applications are currently among the most widely deployed solutions in the industry. The MK6 represents its most advanced, versatile, and powerful platform to date. Thanks to its dual concurrent V2X technology capability, the MK6 provides the reliability, flexibility, and interoperability required for large-scale deployments. For the implementation of the experimental setup, a Cohda MK6 On-Board Unit (OBU) was used. The MK6 is Cohda Wireless' sixth-generation V2X device featuring dual V2X technology support. In our case, it is equipped with Release 19 of the i.MX8 firmware. The main hardware connectivity components include:

- Application Processor i.MX8 (8544 DMIPS)
- DSRC with 2x NXP RoadLink® SAF5400 chipset
- C-V2X with Qualcomm SA515 chipset supporting 3GPP R15, 5G

Figure 3.1: Choda Wireless MK6

- Cellular 5G NR with 4G (LTE Cat 19)/3G/2G fall back
- Wi-Fi (802.11a/b/g/n/ac) 2.4/5 GHz Dual-Band 2x2
- Bluetooth v5.1
- Ethernet (10BASE-T/100BASE-TX/1000BASE-T)
- CAN-FD (up to 5 Mbps)
- Automotive Ethernet (100BASE-T1)
- GNSS receiver – U-Blox M9N

The MK6 uses two independent sources to obtain position and timing information, as it supports both DSRC and C-V2X operation. It relies on the u-blox M9v GNSS receiver for general positioning and timing, while the GNSS module integrated within the Quectel AG550 C-V2X module is used specifically for C-V2X radio operation. The GNSS antenna connected to the MK6 provides the satellite signal to both modules. The Quectel AG550 C-V2X module is based on the Qualcomm SA515M chipset (AEC-Q100 compliant). Adopting 3GPP Release 15 technology, the module supports data rates of up to 2.4 Gbps downlink and 550 Mbps uplink in 5G NSA

mode, and up to 1.6 Gbps downlink and 200 Mbps uplink in LTE-Advanced mode. It also supports direct C-V2X PC5 communication (Mode 4).

For C-V2X transmissions, the base protocol requires strict timing from GNSS because radio transmission in C-V2X mode is time-slot based. Packets are sent in 1ms time-slot and so the timing has to be perfectly synchronised between all the devices operation within the commuication region. for this reason Time synchronization in the Cohda MK6 is achieved through the PPS (Pulse Per Second) signal provided by the GNSS receiver. In this configuration, the synchronization error is on the order of a few nanoseconds. If the 1PPS signal is not available, the system can be configured to synchronize its time to UTC via an external source, such as an NTP server, by modifying the chrony configuration. The MK6 includes an integrated Real-Time Clock (RTC), backed up by a gold capacitor capable of maintaining the RTC for approximately 20 days. At boot-up, the system time is initially retrieved from the RTC and subsequently synchronized with GNSS time through chrony as soon as GNSS data becomes available.

```
 * Documentation:  https://support.cohdawireless.com
Last login: Wed Feb 18 14:28:07 2026 from fe80::7f68:7ecb:ba30:356a%eth0
root@MK6:~# chronyc tracking
Reference ID    : 50505300 (PPS)
Stratum         : 1
Ref time (UTC)  : Wed Feb 18 14:46:21 2026
System time     : 0.000000190 seconds slow of NTP time
Last offset     : -0.000000082 seconds
RMS offset      : 0.000000109 seconds
Frequency       : 72.840 ppm slow
Residual freq   : -0.000 ppm
Skew            : 0.019 ppm
Root delay      : 0.000000 seconds
Root dispersion : 0.000004 seconds
Update interval : 2.0 seconds
Leap status     : Normal
```

Figure 3.2: Synchronization of Cohda MK6 via PPS

3.2 Experimental C-V2X board

This prototypal board integrates the Raspberry Pi Compute Module 3 (CM3) as the main computational unit and the AG15 module for C-V2X communication. The Compute Module 3 is a compact processing unit designed to be integrated into electronic devices and embedded systems. It uses the same Broadcom BCM2837 processor found in the Raspberry Pi 3, a quad-core ARM Cortex-A53 running at 1.2 GHz, and it is equipped with 1 GB of RAM. The prototypal system used in this work also integrates the AG15 i.MX6Q C-V2X module, a platform developed for vehicular communication applications based on C-V2X technology. This module combines an NXP i.MX6Q processor with the Quectel AG15 modem, enabling the execution of telematics applications and cooperative communication between vehicles,

infrastructure, and other connected devices. From an architectural perspective, the system consists of two main units: the i.MX6Q processor, responsible for data processing and application execution, and the AG15 module, which manages C-V2X communication and GNSS functionalities.

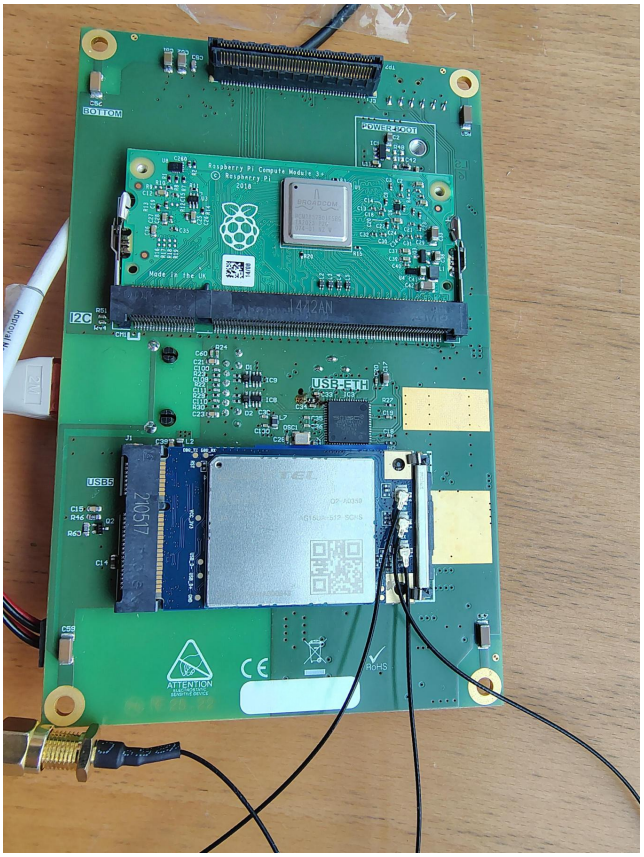

Figure 3.3: prototypal board

3.3 The DriveX OBU

The OBU project, first presented in [3], aims to design and implement a fully functional, open-source, plug-and-play On-Board Unit that can be easily installed on existing vehicles for research and experimental purposes. The system is based on APU2 boards equipped with 4 GB of RAM and runs OpenWrt-V2X as its operating system. The proposed solution is built upon four main design principles:

- Plug-and-play, per facilitare l'installazione su veicoli non connessi;
- Multi-stack, per integrare diverse tecnologie di accesso nello stesso dispositivo;
- Low cost, per offrire un'alternativa economica rispetto alle soluzioni commerciali;
- Open stack, grazie a un'implementazione open source in C++ dello stack ETSI C-ITS.

Figure 3.4: The OBU project

The most relevant design principle is the plug-and-play approach, especially considering that the penetration of V2X technology in the European market is still limited. Many use cases, such as Collision Avoidance, require a significant percentage of connected vehicles in order to be effective. Currently, only a small number of vehicles are equipped with integrated V2X capabilities. For this reason, the project aims to provide an open, cost-effective, and easily installable aftermarket solution, suitable both for research purposes and for fostering a higher technology adoption rate. From a hardware perspective, the OBU is based on PC Engines APU2C4 boards running the latest version of OpenWrt-V2X (21.02.1), a specialized adaptation of the OpenWrt Linux operating system that supports communication over IEEE 802.11p at 5.8/5.9 GHz [49], along with compatible modules such as the selected Mikrotik R11E-5HND. Furthermore, it is equipped with a Sierra Wireless AirPrime MC7455 LTE module, which allows the device to access the internet through the board itself. This provides the possibility of remote access even when the system is no longer within Wi-Fi range. The system also integrates a lane-level accuracy Multi-GNSS receiver connected via USB 3.0. Since standard GNSS accuracy (2–3 meters) may not be sufficient for safety-critical applications, the platform supports differential correction techniques such as Real-Time Kinematic (RTK), enabling centimeter-level positioning accuracy through corrections received, for example, over a cellular network. Each APU2 board interfaces with an ArduSimple simpleRTK2B-F9R device, based on the dual-band u-blox ZED-F9R chipset, supporting update rates of up to 30 Hz and RTK corrections via an NTRIP module over a 4G network. The chipset also integrates an IMU, which provides acceleration data and enables dead reckoning through sensor fusion, ensuring position estimation even in case of GNSS signal loss (e.g., inside tunnels). In addition to standard positioning data, the device

provides raw GNSS measurements, enabling advanced cooperative positioning applications. If connected to the internet, the kernel time synchronization is instead performed via NTP.

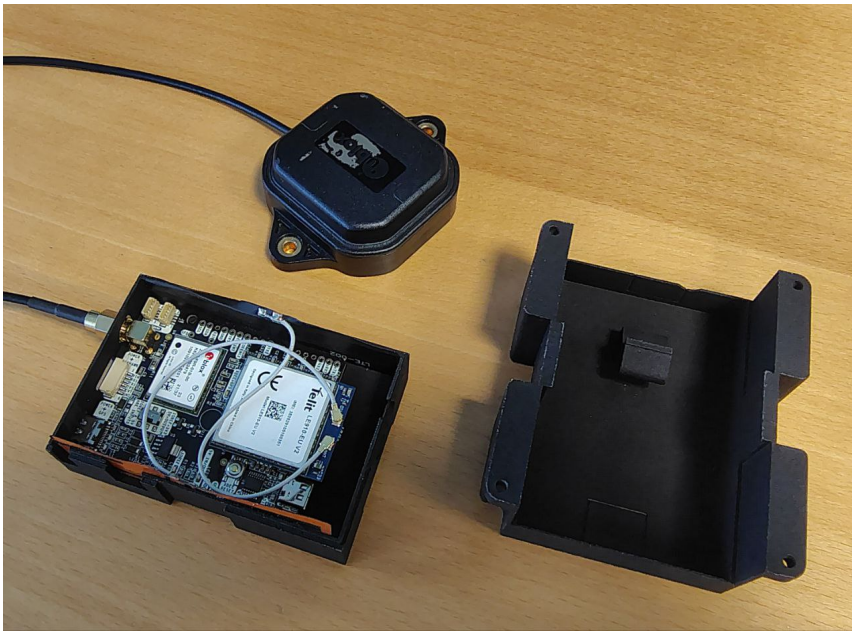

Figure 3.5: simpleRTK2B-F9R

Chapter 4

Software solutions for assessing IEEE 802.11p and C-V2X coexistence

To establish the appropriate environment for the development of software focused on the main metric under investigation, namely latency, the Cohda Wireless platform was selected as the primary development environment. This choice was motivated by its greater maturity compared to the APU2 platform. Furthermore, it supports the transmission of CAM, DENM, MAP/SPAT, and IVI messages and manages the protocol stack for multiple markets, including the European, Chinese, and U.S. regions. The OBU manufacturer provides the SDK as a virtual Linux PC environment in which all development tools and the necessary libraries for a 64-bit ARM processor are pre-installed. The OBU software is primarily written in C or C++, and the Eclipse IDE, equipped with the appropriate plug-ins for these languages, is available for development activities. From the outset, the APU2 boards and the prototype board were designated exclusively for the potential reception of messages and for the computation of latency-related metrics in DSRC and C-V2X environments, respectively. After selecting the embedded solutions, the first step was to determine which types of packets would be used to measure latency. It was firmly decided to rely on messages standardized by ETSI in order to obtain results that are as realistic as possible. The Cohda environment is capable of handling the transmission and reception of the main standardized messages.

The most straightforward choice would have been to use CAM messages, as they are supported by Oscar [49] and could therefore be exchanged without significant effort by the APU boards as well. However, the structure of these messages cannot be freely modified.

Length[byte]	Field		
1	messageId (0=CAM, 1=DENM)		
8	generationTime		
4	StationId		
1	StationCharacteristics	mobileITSStation	
1		privateITSStation	
1		physicalRelevantITSStation	
8+8+4	ReferencePositon	Longitude/Longitude/Elevation	
4		Heading	
32+4		Streetname/RoadSegment ID	
1		Position/Heading Confidence	
1	CamParameters	vehicleCommonParameters	vehicleType
2+2			Length/Width
4			Speed
2			Acceleration
1			AccelerationControl (break, throttle, ACC)...
1			exteriorLights
1			Occupancy
1+1			crashStatus/dangerousGoods

Figure 4.1: CAM structure

Another option that was considered was the use of DENM messages. The fields within these messages are constrained to predefined value ranges depending on the specific parameter. The fields capable of accommodating the widest range of values are those related to geolocation; however, this makes it impossible, when necessary, to track movements through those fields. Below, fragments of the ASN.1 representation are provided.

```
ReferencePosition ::= SEQUENCE {
 latitude Latitude,
 longitude Longitude,
 positionConfidenceEllipse PosConfidenceEllipse ,
 altitude Altitude
}

Longitude ::= INTEGER {oneMicrodegreeEast (10), oneMicrodegreeWest (-10),
unavailable(1800000001)}(-1800000000..1800000001)

Latitude ::= INTEGER {oneMicrodegreeNorth (10), oneMicrodegreeSouth (-10),
unavailable(900000001)}
```

```
(-900000000..900000001)

Altitude ::= SEQUENCE {
 altitudeValue AltitudeValue,
 altitudeConfidence AltitudeConfidence
}

AltitudeValue ::= INTEGER {referenceEllipsoidSurface(0), oneCentimeter(1),|
unavailable(800001)} (-100000..800001)



DeltaAltitude ::= INTEGER {oneCentimeterUp (1), oneCentimeterDown (-1),|
unavailable(12800)} (-12700..12800)
```

The final and ultimately preferred option was the adoption of IVIM messages. As previously stated, IVIM is the message used for the communication of the IVI service, which enables the exchange of road information between an ITS infrastructure and a vehicle. These messages contain a mandatory section of fields that must be correctly populated. In addition, the portion of the structure carrying the actual data required for the proper use of an IVIM is organized in a vector-like form composed of different types of container structures. The number and type of containers can be modified, making the overall IVIM message structure highly flexible and therefore particularly well suited to our purposes. However, the main drawback is that this message type is not supported within the Oscar environment, which consequently required the identification of an alternative solution to enable the reception of such messages on both boards dedicated to this task.

4.1 IVIM generation on Cohda SDK

The IVI Structure is designed to be encapsulated within a message including an appropriate ITS Common Header (e.g., the ItsPduHeader). The structure comprises three main types of containers:

- **Management Container (mandatory)** It is always present and contains information valid for the entire IVI Structure. It provides the receiving ITS Station with the necessary elements to correctly manage and process the message.
- **Location Container (one or more)** It describes the localization information required by the receiving ITS-S applications. The same geographical area may be expressed using different reference systems, allowing the receiving station to use the one it supports. The zones defined in the Location Container are then referenced by the Application Containers.

- **IVI Application Container (one or more)** It contains the application-level information (e.g., limits, restrictions, warnings). It is self-contained from an informational perspective but refers to the spatial zones defined in the Location Container for geographical validity. Application Containers of the same type referring to overlapping zones are not permitted.

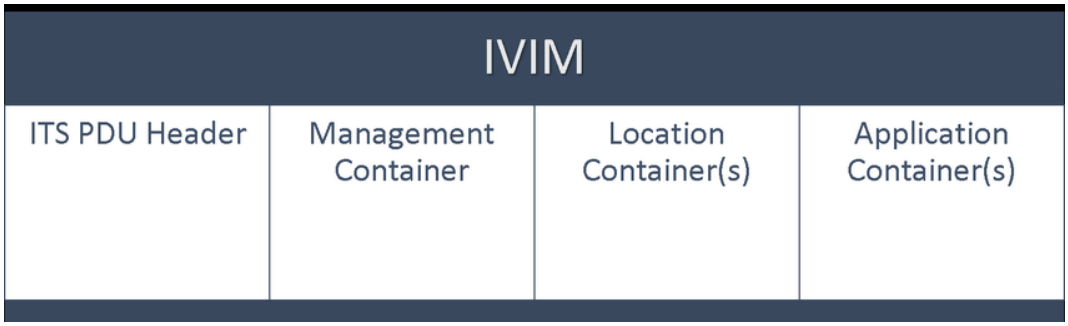

Figure 4.2: IVIM structure

As previously stated, the IVIM is a message designed for the communication of road-related information between an ITS infrastructure and a vehicle.

The IVI Management Container contains the information necessary to manage the lifecycle of the IVI Structure and enables the receiver to determine how the message should be processed. Mandatory components are: *serviceProviderId*, which identifies the organization providing the IVI; *iviIdentificationNumber*, a unique identifier of the IVI Structure assigned by the Service Provider; *iviStatus*, which indicates the state of the IVI Structure (e.g., new, update, cancellation, negation). Optional fields include: timeStamp, validFrom, validTo, connectedIviStructures and connectedDenms.

The IVI Structure may include one or more Location Containers, which provide the spatial information required by the Application Containers. Two types of Location Container are defined: Geographic Location Container (GLC), which represents the main structure of the IviContainer data type, and Map Location Container (MLC), which is an extension of the IviContainer data type. The GLC consists of a common part containing a Reference Position and one or more additional parts defining zones relative to that position.Situation-specific IVI information is contained within one or more Application Containers. The document defines six types: General IVI Container, Road Configuration Container, Text Container, Layout Container, Automated Vehicle Container, and Road Surface Container.

When the application is executed, it relies on two configuration files: a `.cfg` file and a `.conf` file. The `.cfg` file contains the application configuration parameters. It enables the various services of the facilities layer and allows different types of messages to be configured for transmission and reception. In our case, IVIM transmission is enabled and parameters such as the transmission period, the reference position (if a fixed position is selected instead of real-time GNSS), message ID, Service Provider ID, and several others are defined. The Cohda application must therefore correctly handle the different settings specified in this configuration file.

```
ITS = {
  Facilities = {
    IVI =  {
      Enabled = true;
      ApplInterval = 200;

      IVS =  {
        Enabled = true;

        IviIdentificationNumber = 1;
        ServiceProviderRaw = 0xC70001;

        ValidFrom = 0L;
        ValidTo = 0L;
        RefPositionSource        = 0;     # 0=use current GNSS position
                                          # 1=use config position,
        RefLatitude              = -349084140;
        RefLongitude             = 1386064720;
        RefAltitude              = 800001;
        DetectionZoneAbsolutePos =
        (
          {Lat = -349084140, Long = 1386064720},
          {Lat = -349081100, Long = 1386062320}
        )

        RelevanceZoneAbsolutePos =
        (
          {Lat = -349084140, Long = 1386064720},
          {Lat = -349087010, Long = 1386066930}
        )

        GIC =
        (
        {
```

Figure 4.3: Part of the IVIM message configuration contained in the .cfg file.

The `.conf` file is used to override the default stack configuration parameters. It allows modification of radio parameters for G5 (DSRC) transmission, such as transmission power and channel selection, and also enables modification of parameters related to GeoNetworking. Therefore, this file allows the selection of the technology to be used, LTE-V2X or DSRC, for message transmission.

The radio configuration related to C-V2X, such as frequency, channel number, or the Resource Reservation Interval, is defined in a configuration file named `v2x.xml`. However, modifying this file is not straightforward, as it is encoded as a hexadecimal string. To modify this file, a dedicated application was developed that uses the ASN.1 file provided by Qualcomm to adjust these parameters. For example, as shown in the fragment below, the channel is selected through the EARFCN (E-UTRA Absolute Radio Frequency Channel Number):

```
carrierFreq-r12              ARFCN-ValueEUTRA-r9,
```

```
#C-V2X
ItsG5Enabled = 0;
ItsPC5Enabled = 4;
ItsGnIfType  = 2;
```

Figure 4.4: C-V2X configuration for message transmission.

For converting EARFCN to frequency in MHz, the formula is:

$$\text{Center Frequency (MHz)} = 5855 + \frac{\text{EARFCN} - 54540}{10} \tag{4.1}$$

Subsequently, through the calculation shown in (2.1), it is possible to derive the channel number on which transmission occurs.

For the final objective, namely latency evaluation, an absolute time reference comparable across different devices is required, i.e., Epoch time, defined as the number of seconds elapsed since January 1, 1970, 00:00:00 UTC.

The timestamp provided by the IVIM standard within the Management Container is not sufficiently precise. In order to obtain optimal results, a time value comparable at the microsecond level is required. By using the *gettimeofday()* function, which returns two values — one representing seconds and the other the fractional part in microseconds — such precision can be achieved.

The seconds and fractional (microseconds) components returned by *gettimeofday()* are inserted into the latitude and longitude fields of a GLC. While these fields are defined by the standard as 64-bit values, in this implementation the embedded time information is intentionally represented using only 32 bits for each component. As shown in Figure 4.5, the fractional part — consisting of only six digits — can safely be represented within 32 bits. Likewise, the seconds value can also be contained within 32 bits for several decades, provided appropriate masking techniques are applied. This approach does not modify the standard field definition itself, but rather exploits the available bit space to encode the required timing information efficiently, allowing greater flexibility in controlling the effective message size.

To evaluate packet loss and, if necessary, trace transmitted messages, a value representing the sequential index of each generated message is required. This allows identification of missing messages, together with the positional values inserted into the corresponding GLC fields.

According to the standard, when the ITS Station application requests the transmission of IVI information, the service generates and transmits a new IVIM with `iviStatus = "new"`. If the content is modified (for example, by the Service Provider), the ITS-S provides the updated information to the IVI service, which generates an IVIM with `iviStatus = "update"`. Between two consecutive updates, the IVIM

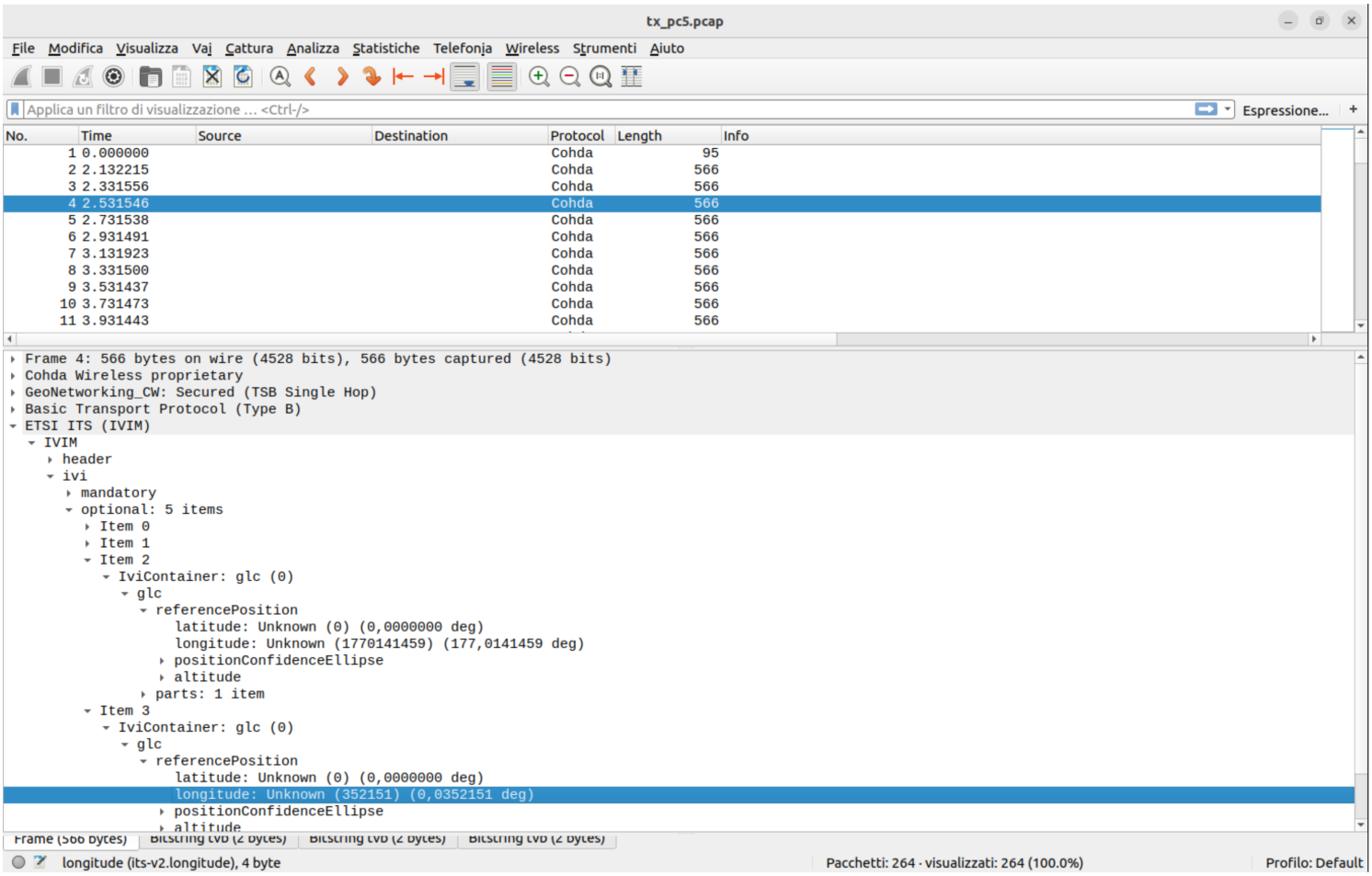

Figure 4.5: Example of a transmitted IVIM message extracted from the .pcap file.

must be retransmitted at predefined intervals so that new ITS Stations entering the validity area can receive it.

In this work, however, the IVIM was required to behave similarly to a CAM message, i.e., to generate a new message periodically. Since no external application dynamically modified the actual IVI content, it was necessary to adapt the transmission logic.

Specifically, the control enforcing `iviStatus = "new"` was bypassed, forcing the generation of a new IVIM at each transmission interval. This ensures that each transmitted message contains updated data for measurement purposes, rather than repeatedly retransmitting identical content.

4.2 IVIM reception

As previously mentioned, the boards responsible for message reception are not capable of directly handling IVIM messages. Therefore, a dedicated application was required to process them. Messages received on the network interface responsible for V2X communication are forwarded to the application through a socket. The application exploits the fact that an IVIM message begins with the byte sequence `0x02 0x06`.

Since the transmitted messages have a fixed and known size, it is possible to extract the entire IVIM payload deterministically. The message is then parsed into its individual fields using the ASN.1 definitions and the Python `asn1tools` library, resulting in a lightweight parser specifically developed for our experimental purposes.

Time Synchronization Issue

Another fundamental aspect for latency evaluation concerns time synchronization between the boards. Neither board supports PPS (Pulse-Per-Second) synchronization. Instead, both rely on the Network Time Protocol (NTP), which synchronizes clocks over IP networks but typically introduces errors on the order of a few milliseconds. This level of accuracy is insufficient for microsecond-level latency measurements.

To overcome this limitation, rather than attempting strict clock synchronization between the two boards, an alternative approach was adopted: exploiting fields from GNSS messages to obtain highly accurate timing information with nanosecond-level precision.

Using the `simpleRTK2B-F9R` GNSS module, it is possible to receive UBX protocol messages relevant to our purposes. The module is connected via USB; after configuring the serial communication parameters, only NAV-PVT messages were enabled in order to minimize serial traffic.

The UBX-NAV-PVT (Position, Velocity, Time) message is the most comprehensive one: it provides geographic coordinates (latitude, longitude, height), three-dimensional velocity components, precise timing information, and GNSS fix quality indicators. A dedicated parser was implemented to process these messages and extract the GNSS time value required for software-level synchronization.

These messages can be received periodically in GET mode or upon request in POLL mode. However, on-demand requests return the most recent message previously generated periodically by the u-blox module, making this mode unsuitable for our purposes. Therefore, NAV-PVT messages were received periodically, and the kernel timestamp corresponding to their arrival was recorded.

When a new IVIM message is received, the arrival time of the IVIM is compared with the arrival time of the most recent NAV-PVT message. This provides an estimate of the Age of Information associated with the UBX message. By adding this Age of Information to the GNSS time value, a theoretically accurate estimate of the IVIM reception time can be obtained.

From the application output log, it can be observed that the latency value,

$$\text{latency} = t_{\text{ricezione}} - t_{\text{invio}} \tag{4.2}$$

is far from constant, exhibiting variations that are too significant to be attributed solely to the transmission channel. This behavior may partially be due to the serial connection between the `simpleRTK2B-F9R` module and the receiving boards, introducing stochastic delays caused by differences in hardware and software components managing GNSS signal reception.

n=40, lat=450647335, lon=76593676, tempo di invio=1770132279122325, tempo di ricezione=1770132279144332 , latenza=22007

n=41, lat=450647334, lon=76593673, tempo di invio=1770132279322250, tempo di ricezione=1770132279328159 , latenza=5909

n=42, lat=450647333, lon=76593670, tempo di invio=1770132279522271, tempo di ricezione=1770132279522068 , latenza=-203

n=43, lat=450647333, lon=76593667, tempo di invio=1770132279722314, tempo di ricezione=1770132279729420 , latenza=7106

n=44, lat=450647332, lon=76593663, tempo di invio=1770132279922340, tempo di ricezione=1770132279935905 , latenza=13565

n=45, lat=450647330, lon=76593662, tempo di invio=1770132280122672, tempo di ricezione=1770132280130208 , latenza=7536

n=46, lat=450647330, lon=76593658, tempo di invio=1770132280322355, tempo di ricezione=1770132280334232 , latenza=11877

n=47, lat=450647329, lon=76593657, tempo di invio=1770132280522271, tempo di ricezione=1770132280530666 , latenza=8395

n=48, lat=450647328, lon=76593654, tempo di invio=1770132280722262, tempo di ricezione=1770132280718601 , latenza=-3661

n=49, lat=450647327, lon=76593651, tempo di invio=1770132280922267, tempo di ricezione=1770132280922630 , latenza=363

n=50, lat=450647326, lon=76593649, tempo di invio=1770132281122749, tempo di ricezione=1770132281130963 , latenza=8214

n=51, lat=450647325, lon=76593646, tempo di invio=1770132281322303, tempo di ricezione=1770132281322175 , latenza=-128

n=52, lat=450647324, lon=76593642, tempo di invio=1770132281522303, tempo di ricezione=1770132281516251 , latenza=-6052

Figure 4.6: Excerpt of the prototype board log output.

Adoption of Round Trip Time

Due to the impossibility of obtaining directly comparable timestamps across different boards, the Round Trip Time (RTT) was selected as the core metric of this study.

By transmitting and receiving messages on a single board, it becomes possible to measure a time value that is internally consistent according to that board's clock. Furthermore, by sending and receiving IVIM messages directly on the Cohda MK6, which fully supports IVIM handling, an external parser is no longer required. Instead, the application running on the Cohda device was modified to compute latency upon message reception and generate a log file containing the relevant metrics. However, this approach may introduce additional packet loss. For LTE-V2X technology, the prototypal board allows the use of a Qualcomm command, *acme -e*, which implements an echo function by retransmitting onto the network what has just been received, albeit through an event port. This retransmission does not follow the constraints of Semi-Persistent Scheduling and therefore does not respect a fixed Resource Reservation Interval. Moreover, the RTT does not correspond exactly to twice the one-way latency, as it also includes message processing time, namely, the time required for upward and downward traversal across the various ETSI protocol stack layers.

The traversal time of the entire stack was estimated using the LaMP follow-up mechanism, implemented in the LaTe tool and described in Chapter 6. This mechanism sends an additional follow-up message after each server response, containing an estimate of the server processing time. The tests showed an average processing time of approximately 0.18 ms.

Chapter 5

Laboratory test

In order to better study the coexistence between the two technologies, we decided to start with a set of laboratory tests. The tests were designed as follows: IVIM messages are transmitted only using LTE-V2X technology, and the related performance metrics are then computed. DSRC technology, on the other hand, is used to generate interference for C-V2X by simulating VANET networks with different levels of congestion.

This approach allows us to obtain a preliminary understanding of the behavior of C-V2X, enabling us to design field tests in a more targeted way. Unlike the study by Bazzi, which focuses on the Packet Reception Ratio (PRR) [50], in this work we also include an analysis related to the timing between the generation and the reception of the messages. Furthermore, the aforementioned study is conducted in a simulation environment, whereas the experiments described subsequently are performed in a real environment. From this analysis, however, it can be observed that the two technologies coexist more efficiently when packet generation follows a constant periodicity.

5.1 Test setup

For this test we used four boards:

- one choda wireless MK6
- one prototype board
- two APU2 boards (the OBU project) described before

Each of these boards is equipped with Mobile Mark MGWG-313 antennas. This multiband surface-mounted antenna, with three cables, provides two C-V2X elements operating at 5.9 GHz and one GNSS element. The standard cable length is approximately 4.5 meters. This model is configured with GNSS, a satellite navigation system that can operate with several global systems, including GPS, Galileo, GLONASS, QZSS, and BeiDou. Thanks to GNSS, the C-V2X modules can synchronize with millisecond accuracy. Regarding transmission power, the prototype board and the

MK6 are configured at 23 dB, while the two APU boards are set to 24 dB. For the LTE-V2X part of the test, the MK6 board is used only in C-V2X mode and is responsible for transmitting the messages. Specifically, every 100 ms it sends an IVIM message with a size of 566 bytes. The prototype board, thanks to the echo function, retransmits the received message back to the MK6, allowing the correct generation of the output log. The part of the test related to DSRC technology is handled by the two APU2 boards, configured with a data rate of 6 Mbit/s. Traffic generation on the channel is performed using the *iperf* tool. OpenWrt fully supports iPerf. The operation of iPerf is based on a client–server architecture. To perform a measurement, at least two devices connected through a network are required. On one device, iPerf runs in server mode and listens on a specific network port. On the second device, iPerf runs in client mode, establishing a connection with the server and sending a sequence of packets for a certain period of time. iPerf supports different transport protocols, mainly TCP and UDP. With UDP it is possible to manually configure the packet transmission rate, allowing the analysis of network behavior under controlled conditions and enabling the measurement of phenomena such as packet loss. One of the main advantages of iPerf is its configuration flexibility. The user can specify several parameters of the test, such as the transmission duration, packet size, the protocol used (TCP or UDP), the target bandwidth in the case of UDP traffic, and the number of parallel streams. This makes the tool particularly useful for simulating different traffic scenarios and evaluating network performance under various conditions. All transmissions take place on channel 182, with a central frequency of 5910 MHz and a transmission bandwidth of 10 MHz according to the standard. We validated our platform through spectrum analysis. In particular, we selected a MetaGeek Wi-Spy DBx 3 USB spectrum analyzer, coupled with the open source Kismet Spectrum-Tools. Since there was initially no support for the DSRC spectrum at 5.9 GHz, the tool was modified in order to enable the analysis of this band, together with the implementation of several additional features that were not originally available [3]. In Figure 5.1 the correct usage of the 10 MHz channel is verified.

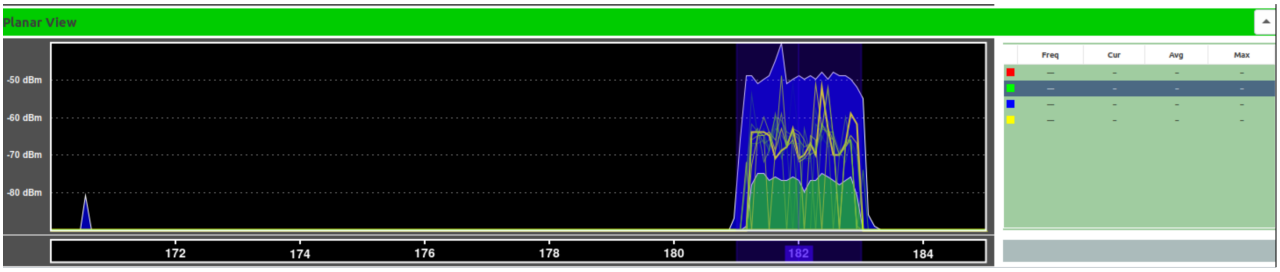

Figure 5.1: Planar view showing the spectrum captured during a test.

One board acts as the client, generating traffic on the channel, which from the C-V2X perspective represents interference. The other board acts as the server, sending an acknowledgment to the first transmission in order to start the iPerf traffic. Furthermore, this board provides useful metrics which, through a dedicated

application developed for this purpose, are extracted using the *iw survey dump* command. This command returns several metrics for different frequencies in the V2X band, such as the *channel active time*, i.e., the total time during which the channel has been monitored, and the *channel busy time*, i.e., the time during which the channel was occupied. For the calculation of the Channel Busy Ratio (CBR), a dedicated program extracts only the metrics related to the frequency with central frequency at 5910 MHz, which is the one used for the transmissions. By computing the ratio between busy time and active time within a time window of 500 ms, it is possible to calculate the CBR. All the boards are connected to a switch, which is in turn connected to my PC, allowing centralized management. In order to manage these tests quickly and autonomously, an application for test automation was required. To automate the tests on the boards, a script was developed that automatically establishes an SSH connection with the four devices. Once the connection is established, the script sequentially sends the commands required to configure the test environment. The application receives as input the SSH passwords of the boards, the minimum and maximum traffic offered by the iPerf client, the number of repetitions for each test in order to average the metrics over multiple runs, and the increment of the offered traffic after completing all tests with the same parameters. Each individual test is executed in the following order:

- the APU2 board acting as server starts the server and launches the application used to compute the CBR
- the prototype board enables the echo function
- the APU client starts sending traffic using iPerf
- the choda MK6 starts transmitting the messages
- after approximately two minutes the echo function is disabled first, in order to maintain a roughly constant number of packets across different tests
- the APU client stops sending traffic through 802.11p and the MK6 stops the transmission of messages
- finally, all generated output files are collected

As a trade-off between the time required to execute the tests and the amount of collected data, the results are averaged over 8 runs for each configuration. In this way, during the two-minute test approximately 1170 packets are generated, resulting in a total of about 9360 packets transmitted by the MK6. These packets are then used to compute latency, packet loss, and the resulting confidence interval.

5.2 Result

As a first analysis, after observing that fully saturating the channel with DSRC leads to the loss of all packets subsequently transmitted using LTE-V2X, we decided

to evaluate the metrics as a function of the traffic generated by iperf. The offered traffic was varied from 0 to 10 Mbit/s with a step of 1 Mbit/s, in order to obtain a coarse overview of the system behavior and identify the regions that required a more detailed analysis. This was done while being aware that, since the board is configured with a theoretical maximum throughput of 6 Mbit/s, corresponding to a real throughput of 4.86 Mbit/s for packets of 1470 B [3], the channel would already be saturated before reaching 10 Mbit/s.

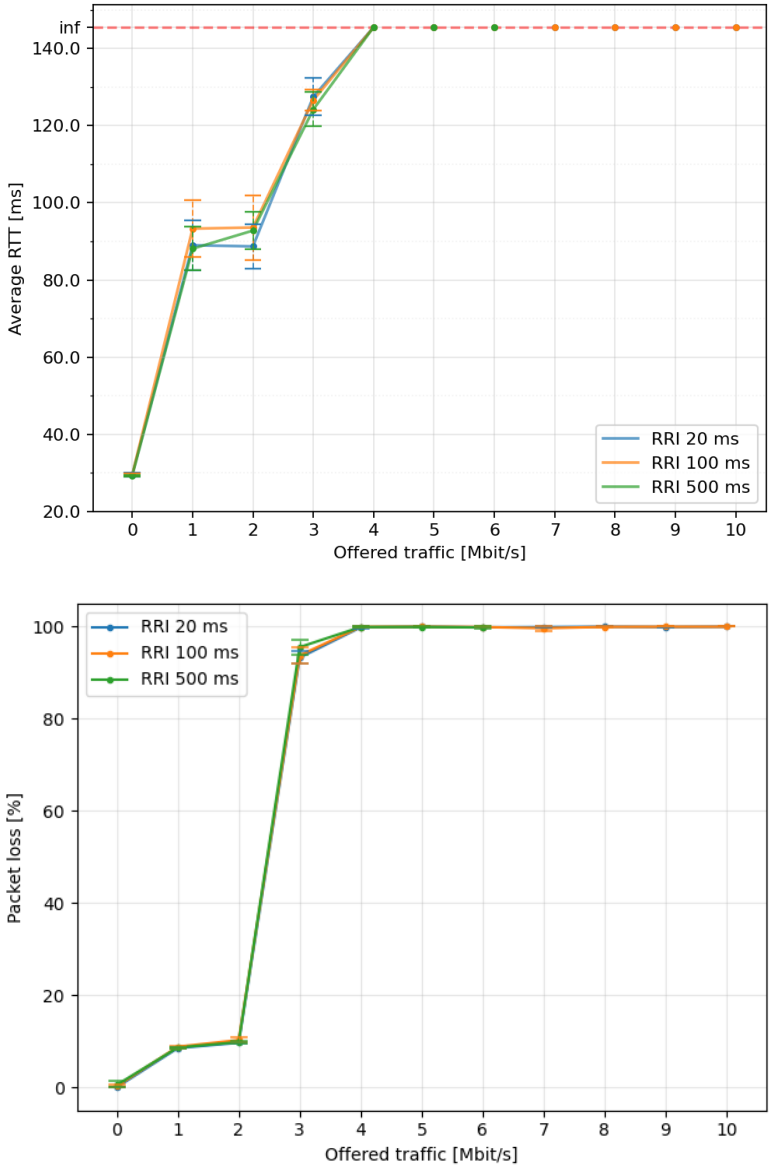

Figure 5.2: Average Round Trip Time (RTT) and Packet loss (PL) as a function of the DSRC traffic generated by iperf between 0 and 10 Mbit/s. The three curves correspond to different RRI configurations (20 ms, 100 ms, and 500 ms). Horizontal error bars represent the 95% confidence interval. The dashed red line indicates the saturation condition where RTT is considered infinite due to excessive packet loss.

In Figure 5.2 it is possible to observe that the average Round Trip Time increases as the traffic generated by iperf increases, up to 4 Mbit/s. Beyond this point, we

consider the RTT to be infinite. By infinite round trip time we mean that packets do not return to the sender, making it impossible to compute the corresponding metrics. In these tests we consider a reception threshold of at least 1% of the transmitted packets in order to calculate a valid RTT value. As shown in Figure **??**, at 4 Mbit/s the Packet Loss (PL) exceeds 99%. It can also be observed that changing the RRI value does not significantly affect the RTT or the packet loss, since the measured values fall within the same statistical range. In particular, all the measurements with RRI set to 20, 100, and 500 ms fall within the same confidence interval, fixed at 95%.

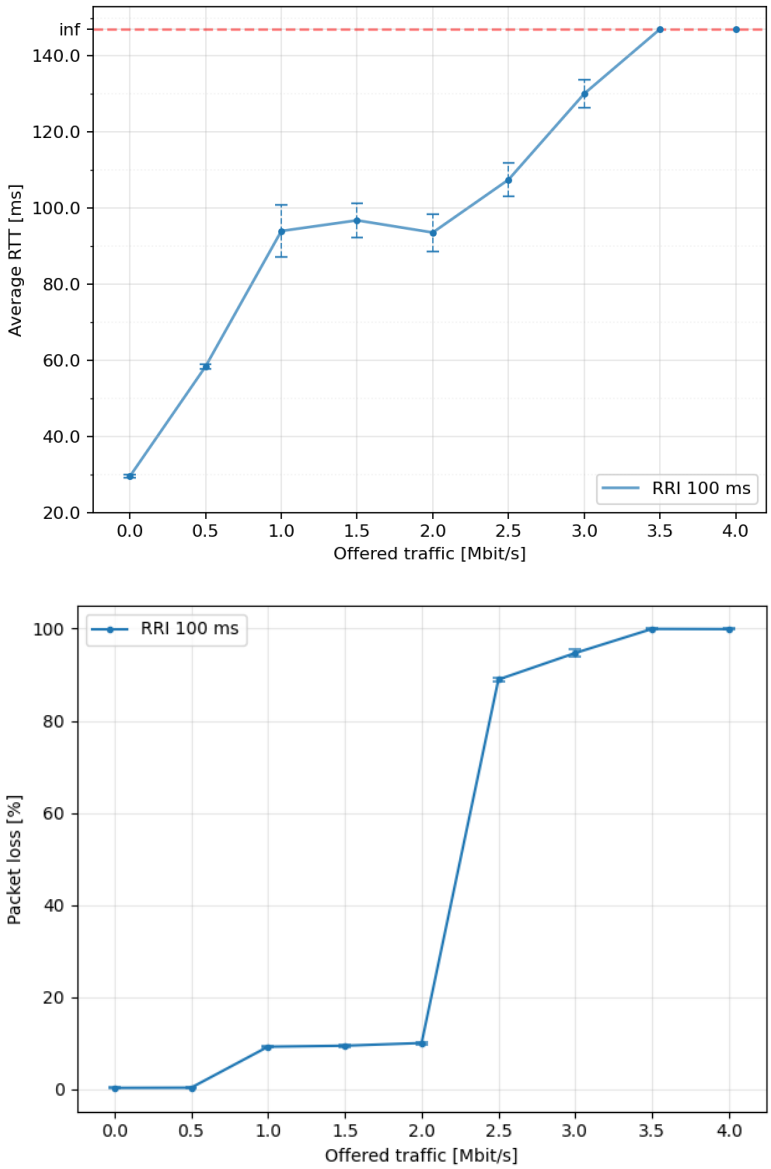

Figure 5.3: Average Round Trip Time (RTT) and Packet loss (PL) versus DSRC traffic generated by iperf between 0 and 4 Mbit/s for RRI = 100 ms. Horizontal error bars represent the 95% confidence interval. The dashed red line indicates the saturation condition.

After verifying that above 4 Mbit/s it is no longer possible to obtain a valid reception of IVIM messages through LTE-V2X, we performed a more detailed test in

the range considered valid. In Figure 5.3, the offered iperf traffic ranges from 0 to 4 Mbit/s with a step of 0.5 Mbit/s between the different configurations. From this analysis it can be observed that a packet loss of 99%, and therefore the impossibility of calculating the RTT, is already reached at 3.5 Mbit/s of offered traffic. Between 0 and 3.5 Mbit/s the RTT shows an almost linear increase, with a relatively flat region between 1 and 2 Mbit/s. This behavior is likely due to the fact that, with this level of offered traffic, corresponding to a certain background interference from the LTE-V2X perspective, the system is still able to find transmission slots for the messages in a relatively stable manner across this range. It should be noted that these results refer to the transmission of ETSI messages of 566 B with a periodicity of 100 ms.

Regarding packet loss, shown in Figure 5.3, it can be observed that the largest increase in packet loss occurs between 2 and 3 Mbit/s. This led us to analyze the corresponding channel occupancy. Figure 5.4 shows the Channel Busy Ratio calculated using the program described previously. As expected, the trend is approximately linear. Furthermore, as anticipated from the throughput analysis, when the offered traffic reaches 2.5 Mbit/s the channel occupancy is slightly below 50%. However, this level of congestion is already sufficient to generate a packet loss higher than 85%. This likely indicates that the OFDM subcarriers of IEEE 802.11p and the LTE-V2X carriers interfere with each other in at least 15% of the transmissions.

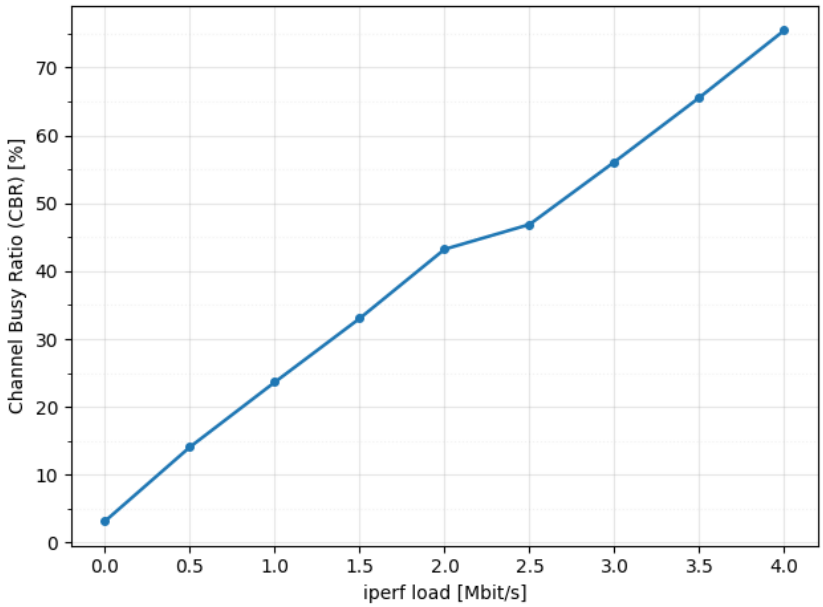

Figure 5.4: Channel Busy Ratio (CBR) measured at 5910 MHz as a function of the DSRC traffic generated by iperf on the IEEE 802.11p channel.

Due to this significant packet loss between 2 and 3 Mbit/s, we performed a final test by setting the offered traffic between 2 and 3 Mbit/s with a step of 0.1 Mbit/s. As shown in Figure 5.5, the average Round Trip Time increases up to an offered traffic of 2.3 Mbit/s. At this point the packet loss also exceeds 55%. For higher values, the trend becomes unstable. This suggests that the reliability of the data

decreases significantly when the packet loss exceeds approximately 55%, especially when comparing very small variations in network congestion. In contrast, in the previous tests the variations were larger and it was therefore easier to observe a clear increase in the packet time of flight.

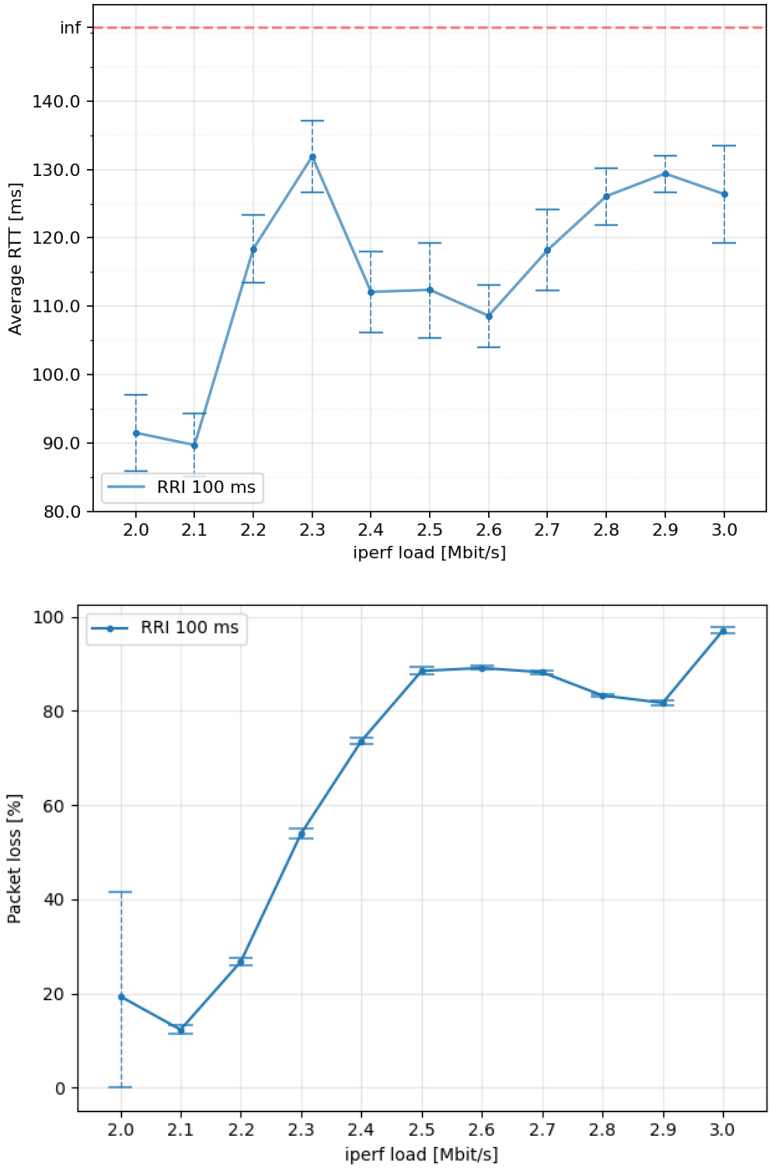

Figure 5.5: Average Round Trip Time (RTT) and Packet loss (PL) versus DSRC traffic generated by iperf between 2 and 3 Mbit/s for RRI = 100 ms. Horizontal error bars represent the 95% confidence interval. The dashed red line indicates the saturation condition.

Chapter 6

Field test

As mentioned previously in this thesis, we will also analyze coexistence in a real environment. The goal is to verify whether the static tests performed in the laboratory are confirmed under real conditions and to compare them with scenarios in which the transmitting vehicles are moving. This allows for a more complete analysis of the coexistence phenomenon between LTE-V2X and IEEE 802.11p.

6.1 Setup

As in the laboratory tests, the same hardware components are used for the field tests. The part of the test related to DSRC technology is handled by the two APU2 boards (the OBU project). For the LTE-V2X part of the test, the MK6 board is used only in C-V2X mode and is responsible for transmitting the messages as in the previous experiments. The prototype board, thanks to the echo function, retransmits the received message back. All the boards are equipped with Mobile Mark MGWG-313 antennas. In addition, the APU2 boards are equipped with the GNSS module simpleRTK2B-F9R.

Figure 6.1: Experimental setup installed on a moving vehicle.

In Figure 6.1, it is possible to see that the moving vehicle is equipped with the Cohda MK6 board and an APU2 with a GNSS module. These are connected to a switch, which in turn is connected to a PC in order to manage and control the devices.

In Figure 6.2, the stationary vehicle is equipped with the prototype board and the other APU2, also paired with the simpleRTK2B-F9R module. The four magnetic antennas are positioned on the roofs of the vehicles, two for each car. Each board is powered by Bresser batteries, with one battery per vehicle.

Figure 6.2: Experimental setup mounted on a stationary vehicle.

Unlike the laboratory tests, no dedicated application was used in this case, neither for the static tests nor for the dynamic ones. The static tests were very short, and in the dynamic tests it would have been difficult to follow predefined timing constraints, since they were carried out on a public road that required maneuvers both at the start and during the return phase.

6.2 Results

6.2.1 Static test

Before performing the dynamic tests, where one of the two vehicles is moving, two sets of static tests were conducted. In the first set, both the interfering traffic generated by *iperf* and the IVIM messages were transmitted on the same channel. In the second set, the two transmissions were performed on adjacent channels.

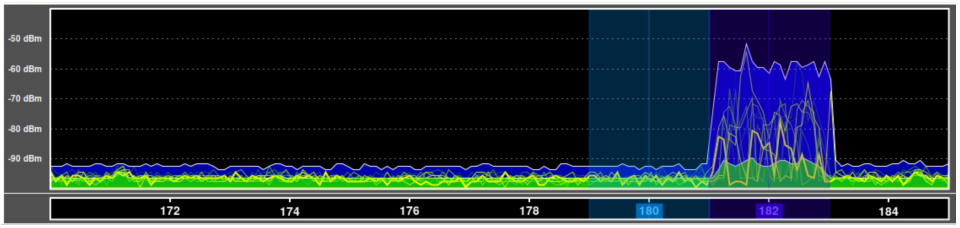

Figure 6.3: Planar view showing the spectrum captured during a test on the 182 channel.

The static tests on the same channel, as shown in Figure 6.3, were performed in order to confirm the results previously observed during the laboratory experiments.

From Figure 6.4 6.5, which shows the Packet Loss (PL) and the Round Trip Time (RTT) as a function of the interfering traffic generated by *iperf*, it can be observed that the graphs follow the same trend as those obtained in the laboratory, although

with slightly higher values, especially in terms of packet loss. This is most likely due to the fact that the previous experimental setup was not reproduced exactly. In particular, the antenna generating the interfering traffic is located on the same roof of the vehicle that transmits the LTE-V2X messages, while the vehicle equipped with the prototype board is positioned approximately 4.7 meters away.

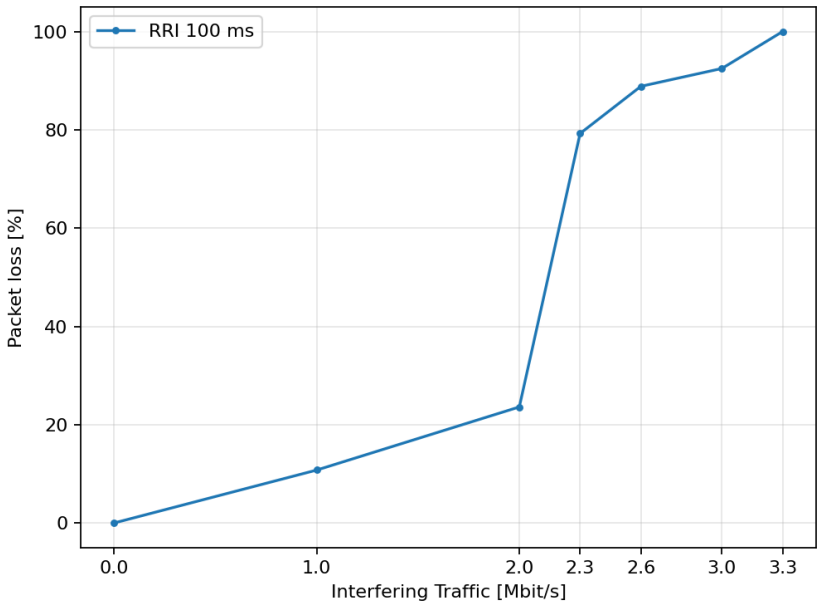

Figure 6.4: Packet Loss (PL) as function of DSRC interfering traffic (0 and 3.3 Mbit/s), with RRI = 100 ms on the same channel.

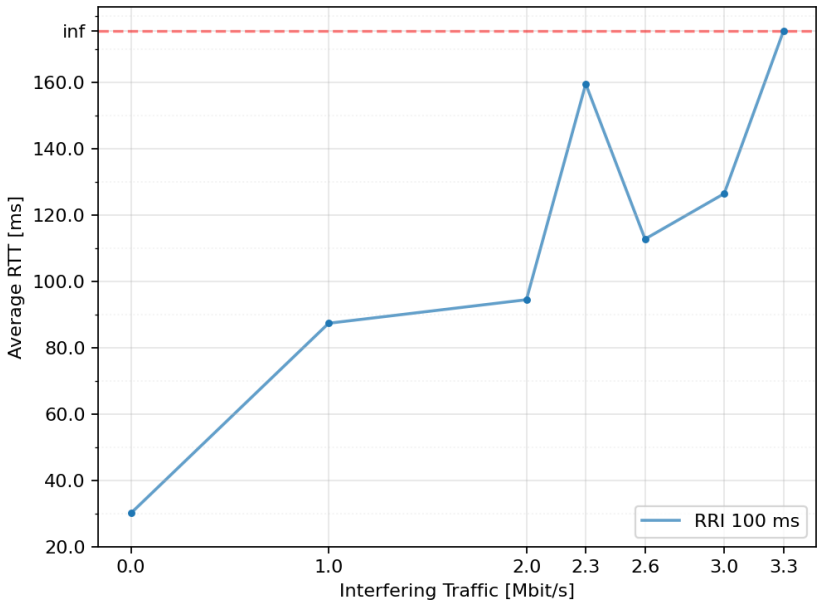

Figure 6.5: Average Round Trip Time (RTT) a function of DSRC interfering traffic (0 and 3.3 Mbit/s), with RRI = 100 ms on the same channel. The dashed red line indicates the saturation condition.

In addition to the static tests with transmissions on the same channel, tests

were also carried out to verify whether transmissions on adjacent channels could cause interference. As shown in Figure 6.6, the trapezoidal-shaped transmission, corresponding to DSRC, is located on channel 180, while the LTE-V2X transmission, characterized by a spike-like shape, takes place on channel 182.

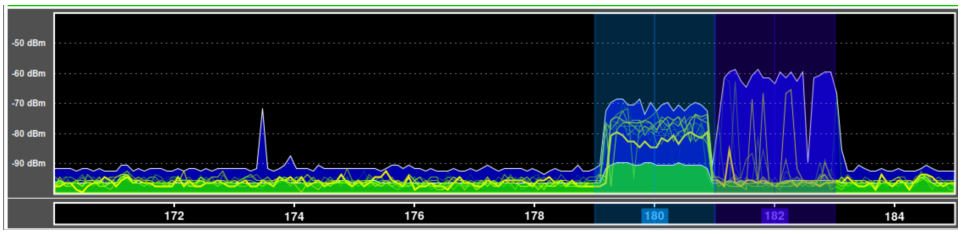

Figure 6.6: Planar view showing the spectrum captured during a test on .

From the graphs in Figure 6.7 6.8, it can be observed that both the Packet Loss and the Round Trip Time increase between 1 and 2 Mbit/s of interfering traffic. After 2 Mbit/s, however, PL and RTT tend to flatten, suggesting that they have reached a saturation value.

This behavior is reasonable, since the interference between the two technologies is likely due to the non-ideal spectral shape of the DSRC and LTE-V2X transmissions. In practice, the signals slightly exceed the nominal 10 MHz bandwidth assigned to the channel, as can be observed in Figure 6.6. Therefore, as the interfering traffic increases and produces a more continuous transmission in those frequency regions, both the Packet Loss and RTT increase. When the transmission becomes even more intense and occupies the entire channel rather than only the spectral leakage regions, these metrics tend to stabilize and reach an approximately constant value.

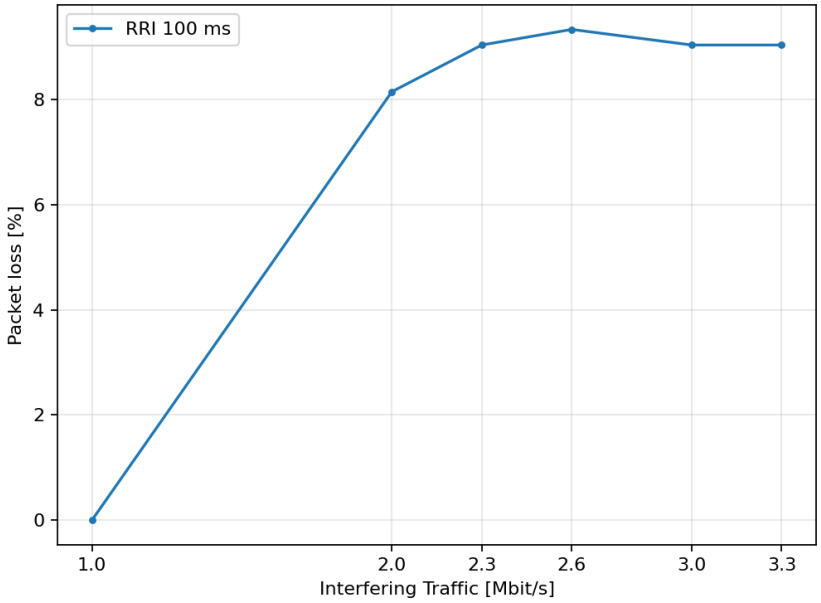

Figure 6.7: Packet Loss as a function of DSRC interfering traffic (0-3.3 Mbit/s), with RRI = 100 ms on adjacent channel.

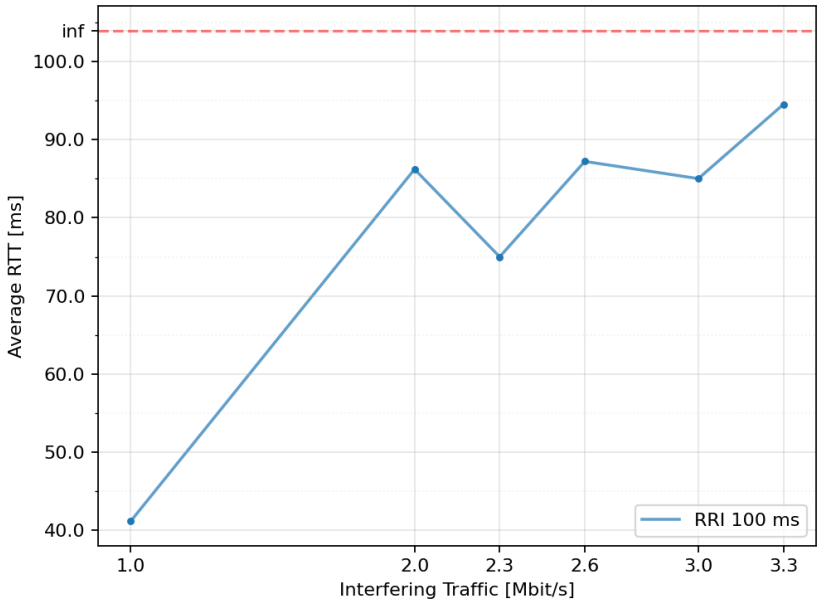

Figure 6.8: Average Round Trip Time (RTT) as a function of DSRC interfering traffic (0-3.3 Mbit/s), with RRI = 100 ms on adjacent channel. The dashed red line indicates the saturation condition.

6.2.2 Dynamic test

LTE-V2X transmission

After completing the static tests, the dynamic tests were carried out. These tests were performed according to the following procedure:

- The moving vehicle, traveling at an average speed of about 60 km/h and equipped as previously described, transmitted IVIM messages using the Cohda MK6.
- The stationary vehicle, on the other hand, generated interfering traffic through the APU2 using *iperf*, while the prototype board used the echo function to send the received messages back to the Cohda board.

This type of test is designed to simulate a realistic coexistence scenario. In particular, a vehicle transmitting messages using LTE-V2X approaches or moves away from an area with different densities of vehicles transmitting through IEEE 802.11p. In these situations, the VANET may experience different levels of channel occupancy, which in the laboratory tests were represented by the relationship between the Channel Busy Ratio (CBR) and the interfering traffic generated through *iperf*.

To evaluate the behavior of Packet Loss and Round Trip Time as a function of distance, the separation between the transmitting vehicle and the stationary one was divided into slots of 30 meters. This approach allows multiple measurements to be collected within the same distance range and makes it possible to compute an average value for each slot. Without this subdivision, the Packet Loss calculation

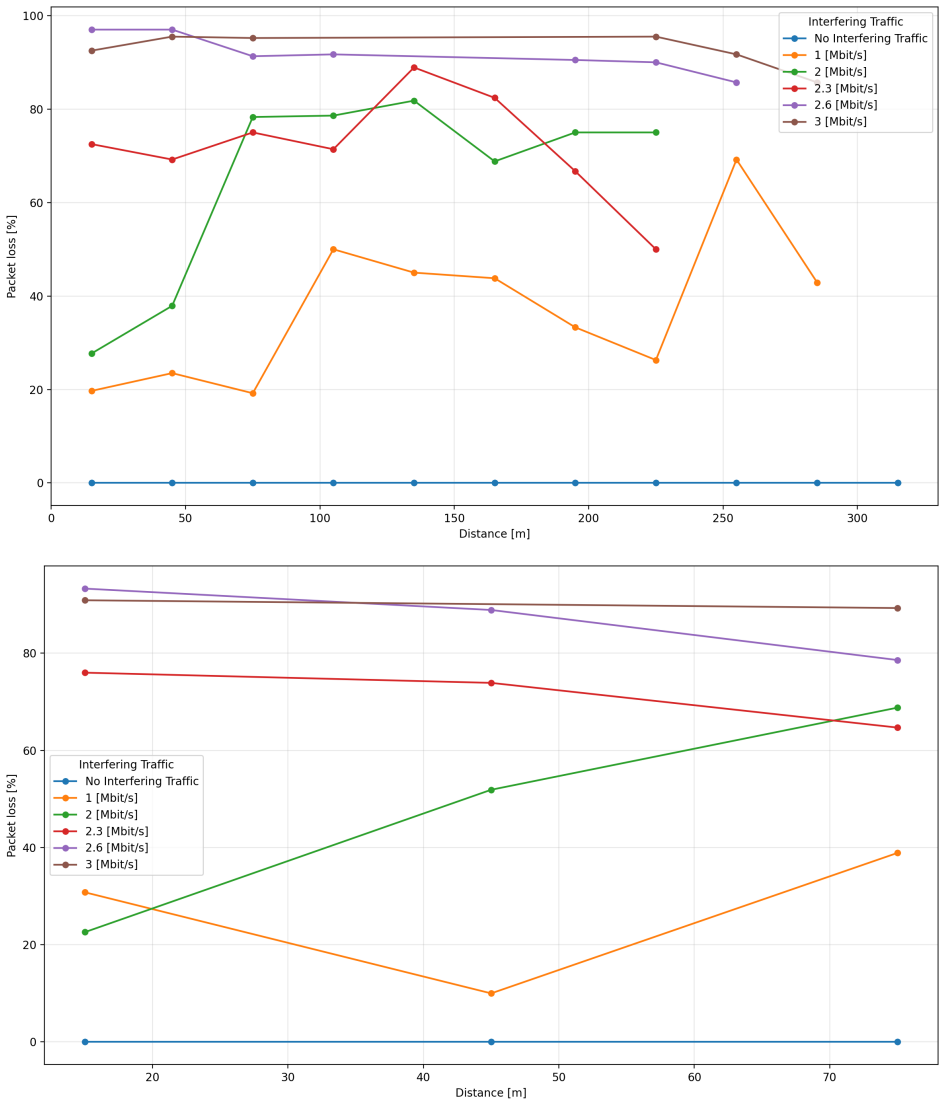

Figure 6.9: Packet Loss as a function of distance under DSRC interfering traffic (0-3 Mbit/s). The first plot corresponds to the vehicles moving apart, while the second corresponds to the vehicles approaching each other.

would not be meaningful, since at a specific distance the result would simply be either 0% or 100%, depending on whether the packet was received or not. In general, it can be observed that the maximum communication distance during the outbound and return phases is different. When the boards are already communicating, during the phase in which the vehicles move away from each other, message exchange with an interfering traffic of 1 Mbit/s can be maintained up to the distance slot of 270–300 m. During the approaching phase, when the communication between the two boards must first be established, the connection begins approximately in the 60–90 m distance slot. Figure 6.9 shows the Packet Loss (PL) during both the separation and the approaching phases between the two vehicles. In general, it can be observed that in both movement phases the Packet Loss increases with both the distance and the level of interfering traffic, except for a few points that are most likely due to the limited amount of data available for the analysis.

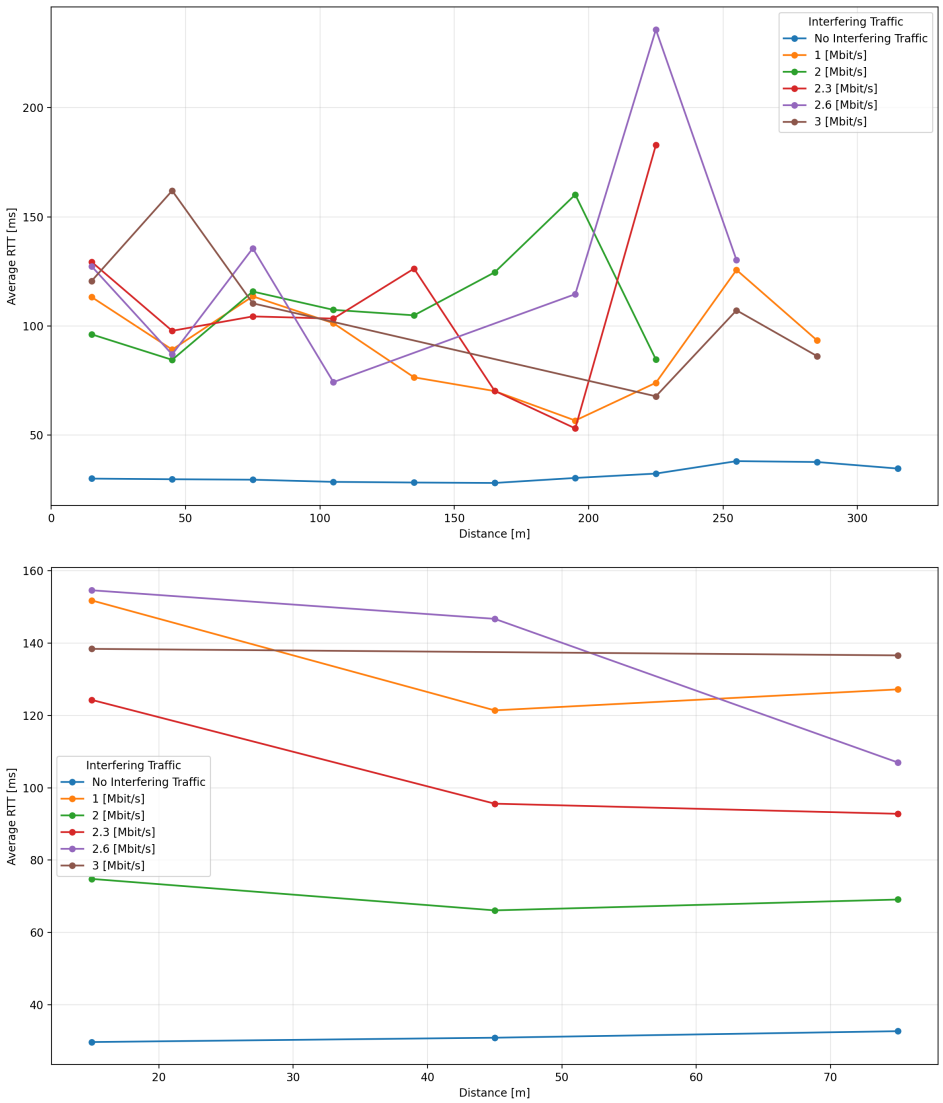

Figure 6.10: Average Round Trip Time (RTT) as a function of distance under DSRC interfering traffic (0-3 Mbit/s). The first plot corresponds to the vehicles moving apart, while the second corresponds to the vehicles approaching each other.

In the outbound graphs shown in Figure 6.10, it can be observed that during the separation phase of the moving vehicle the Round Trip Time exhibits a fluctuating behavior with respect to distance. In addition, the different curves representing different saturation levels intersect with each other. During the return phase, for interfering traffic values generated by `iperf` of 1, 2, and 2.3 Mbit/s, the curves show a similar shape; however, they appear in the opposite order compared to what would normally be expected. In fact, the curve associated with the lowest interference level appears above the others, indicating a higher average RTT. These results may mainly indicate two aspects. First, the dataset available for the analysis may be limited and therefore insufficient for a more detailed evaluation. Second, in the real scenario considered for our tests, the RTT does not appear to show a clear dependency on either the distance or the level of traffic on the channel. This behavior differs from what is observed for Packet Loss, where the relationship with both distance and

interfering traffic is more evident.

Figures 6.11 and 6.12 show the complete dataset, combining the metric values measured during both the separation and the approaching phases. The plots highlight the behavior of RTT and PL as a function of both the distance between the vehicles and the level of interfering traffic through 3D visualizations.

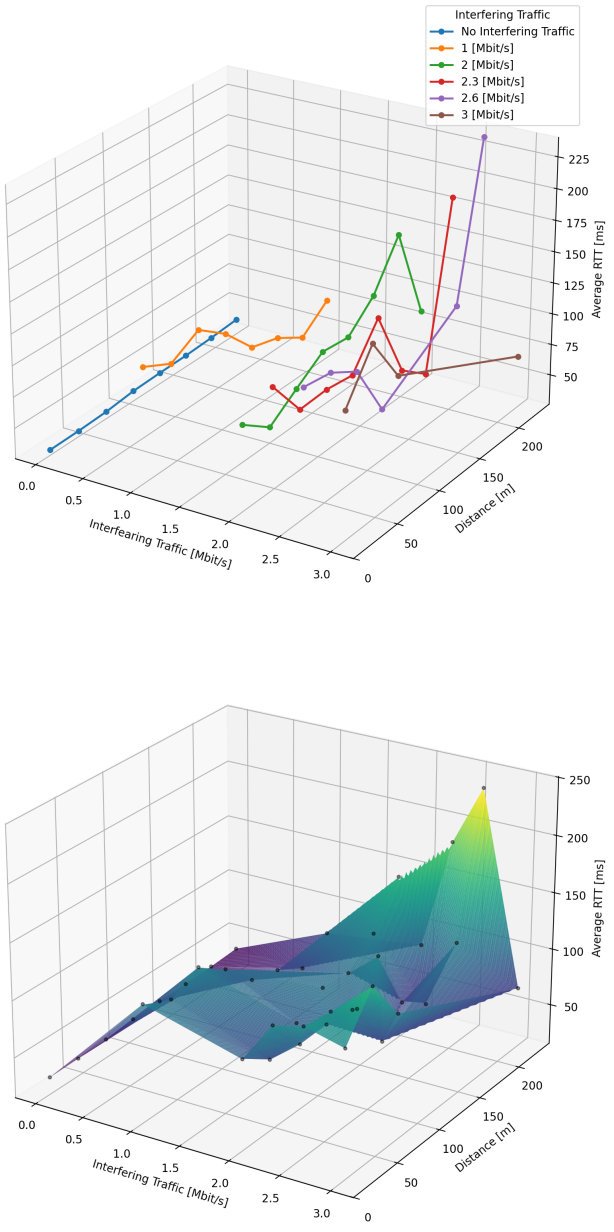

Figure 6.11: 3D visualizations of Round Trip Time (RTT) as a function of DSRC interfering traffic and distance. The first plot shows the curves corresponding to different interfering traffic levels, while the second plot shows the interpolated points forming a 3D surface.

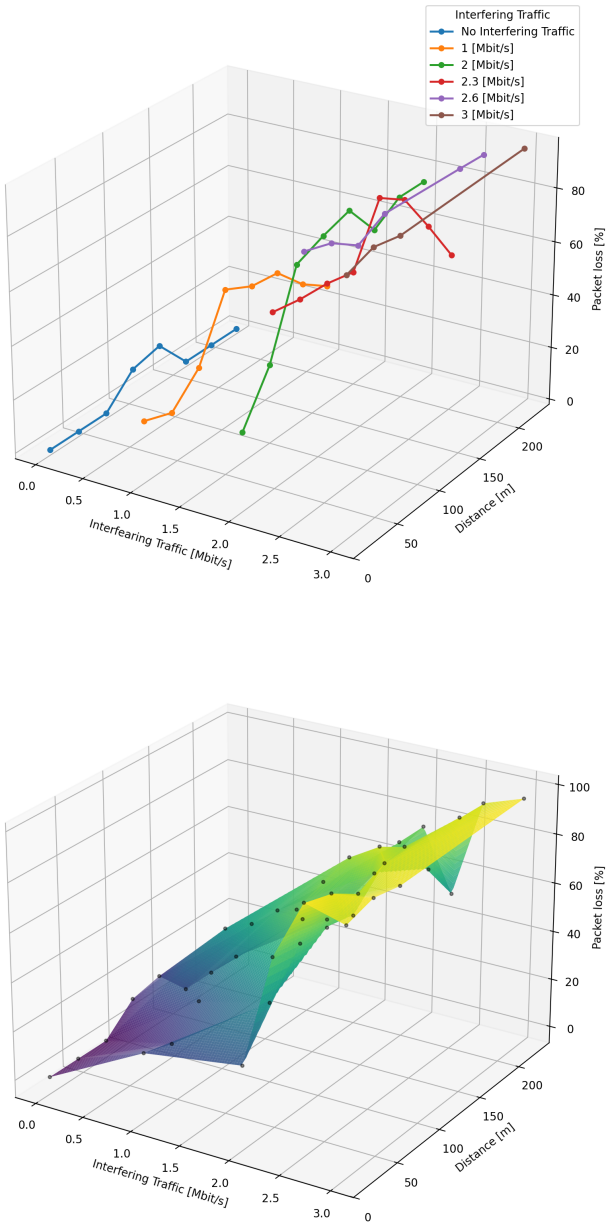

Figure 6.12: 3D visualizations of Packet Loss (PL) as a function of DSRC interfering traffic and distance. The first plot shows the curves corresponding to different interfering traffic levels, while the second plot shows the interpolated points forming a 3D surface.

IEEE 802.11p transmission

To measure the metrics related to the IEEE 802.11p technology, we use LaTe, a tool that allows the simulation and analysis of realistic vehicular communication scenarios. Latency Tester (LaTe) is an open-source tool developed for accurate latency measurements in communication networks, with particular focus on automotive applications and Vehicle-to-Everything (V2X) networks [3].

LaTe is able to measure latency at the application level. This means that the

measurement includes not only the packet transmission time over the network, but also the processing time required by the operating system and the application itself. The tool implements the LaMP (Latency Measurement Protocol), which is designed to be independent of the network layer. Currently, LaTe supports LaMP over UDP, which is particularly suitable for V2X communications, as it enables low-latency transmissions with reduced overhead compared to other protocols.

To simulate interfering traffic produced by LTE-V2X, the only method currently available is to transmit messages at the maximum possible frequency using the Cohda MK6 board and, through the echo function, double the traffic on the channel. With the same configuration used previously, it is therefore possible to generate an interfering traffic of approximately 0.1 Mbit/s.

The setup used for this test is slightly different from the previous one. In this case, the interfering traffic is not generated by the stationary vehicle but moves together with the moving vehicle. This configuration simulates a scenario in which vehicles generating LTE-V2X traffic travel together with the one transmitting IEEE 802.11p messages. The setup is therefore composed as follows:

- The moving vehicle, traveling at a speed of approximately 60 km/h and equipped as described previously, transmits IVIM messages in order to generate interfering traffic. The APU2, which in this case operates as the LaTe client, manages the transmission of DSRC messages and computes the corresponding metrics when the messages are received back.
- The stationary vehicle, through the APU2 and the prototype board, returns the received messages to the sender by acting as an echo node.

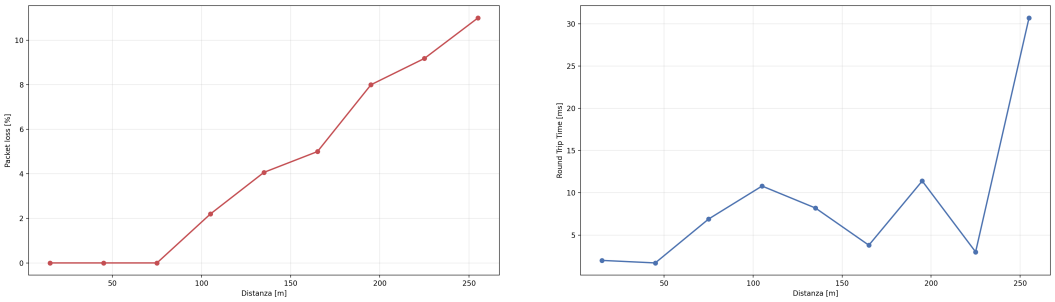

Figure 6.13: Average Round Trip Time (RTT) and Packet Loss (PL) as a function of distance in the presence of LTE-V2X interfering traffic.

In Figure 6.13, which represents the Packet Loss and RTT of packets transmitted through DSRC in the presence of C-V2X traffic, it can be observed that after a certain distance, around 75 m (corresponding to the 60–90 m slot), the Packet Loss begins to increase approximately linearly. The RTT, when observed at a macroscopic level, also increases as a function of distance. However, a more detailed view shows that in some points the RTT slightly decreases; this behavior is mainly due to the progressive increase in Packet Loss.

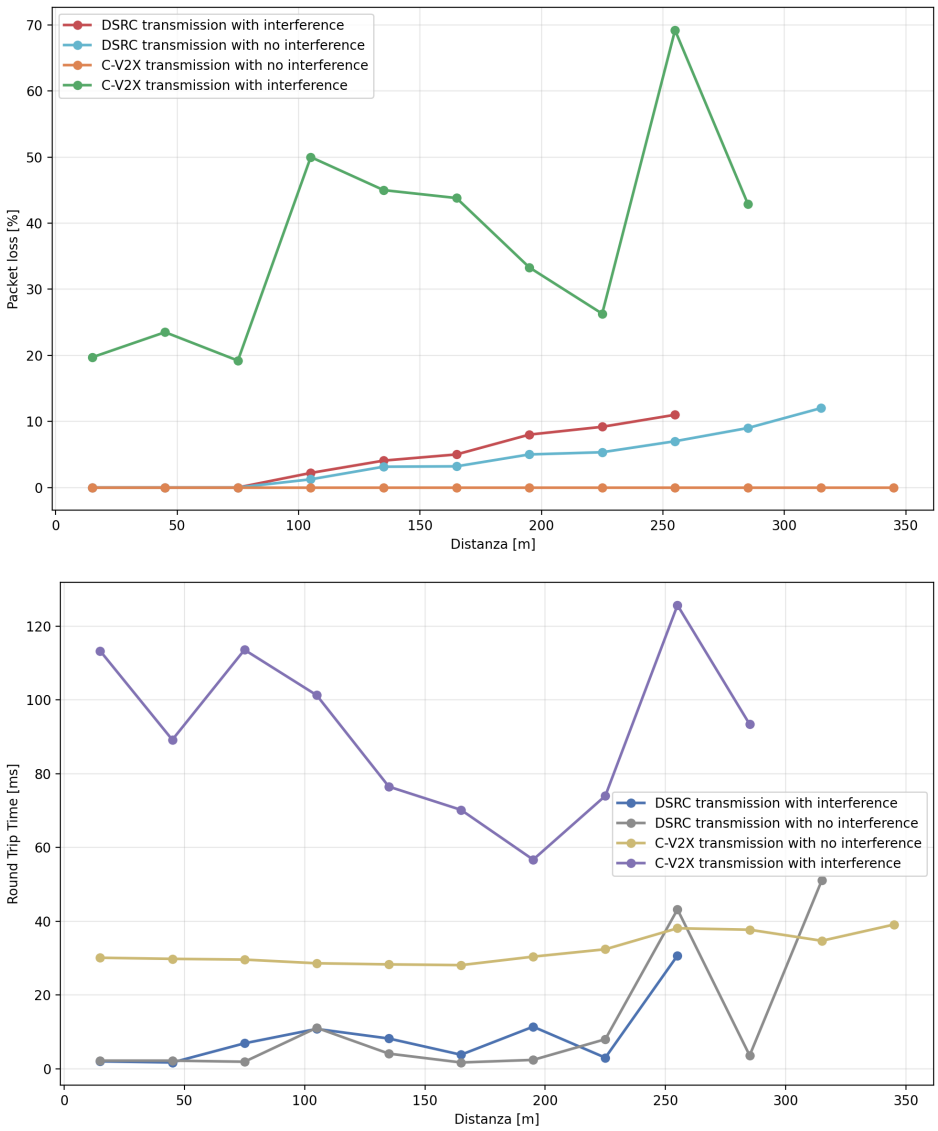

Figure 6.14: Comparison of average Round Trip Time (RTT) and Packet Loss (PL) versus distance for IEEE 802.11p and LTE-V2X transmissions, with and without interference.

In the graphs shown in Figure 6.14, DSRC transmissions with and without interference, measured using LaTe, are compared with LTE-V2X transmissions with interfering traffic at 1 Mbit/s and without interference. The analysis considers only the phase in which the moving vehicle increases its distance from the stationary one.

In general, when comparing the transmissions with and without interfering traffic, LTE-V2X performs better over longer distances. In particular, when interference is present, LTE-V2X reaches the 270–300 m slot, whereas DSRC reaches approximately the 240–270 m slot. It is also important to note that the interfering traffic affecting DSRC is about one tenth of that affecting LTE-V2X. Regarding Packet Loss, as expected, the LTE-V2X transmission in the presence of interfering traffic shows the highest PL among all the considered scenarios, since it is also the case with the highest level of channel load. In other words, the larger amount of interfering

traffic naturally leads to a higher probability of packet loss. DSRC transmissions instead show a roughly linear increase in Packet Loss with distance, with the curve corresponding to the free channel scenario lying below the one obtained in the presence of interfering traffic generated by C-V2X. It is also worth noting that LTE-V2X transmissions without interfering traffic maintain a Packet Loss that remains approximately constant and close to 0% as the distance increases. The Round Trip Time shows a more fluctuating behavior. However, it can be observed that for low interfering traffic values, for example around 0.1 Mbit/s, DSRC tends to achieve lower latency on average. When the C-V2X channel is free of interference, the RTT, similarly to Packet Loss, remains relatively constant as a function of distance.

Chapter 7

Conclusion

In recent years, the development of Intelligent Transportation Systems (ITS) and technologies for assisted and autonomous driving has led to increasing attention toward vehicular communications. Currently, two main technological solutions are considered the most mature candidates for supporting Vehicle-to-Everything (V2X) communications: IEEE 802.11p, which belongs to the Wi-Fi family and is based on the DSRC paradigm, and LTE-V2X, the first release of the so-called Cellular-V2X (C-V2X), developed by the 3GPP and based on cellular network technologies. The lack of a definitive regulatory and industrial choice makes it likely that both technologies will coexist in future deployments, particularly in the European context, where the regulatory approach is technologically neutral. In such a scenario, studying the coexistence between IEEE 802.11p and LTE-V2X becomes essential to understand how these technologies can operate simultaneously in the spectrum dedicated to ITS communications, namely the 5.9 GHz band. The main objective of this thesis has been to analyze the behavior of these two technologies in scenarios characterized by interference and shared traffic, evaluating their performance in terms of latency and packet loss. To achieve this goal, an experimental platform based on dedicated hardware and software components for V2X communications was designed and implemented. The platform was developed using a commercial board, the Cohda MK6, together with other lower-level development boards. The experimental activity was divided into two main phases: laboratory tests and field tests. Laboratory tests were carried out to analyze the coexistence behavior in a static environment. Since these experiments were performed in a controlled setting, it was possible to repeat the measurements multiple times and average the results, thereby reducing statistical error. The obtained results showed that an increase in interfering traffic leads to a significant growth in Round Trip Time (RTT) and packet loss, highlighting the channel saturation phenomenon when the traffic exceeds certain thresholds. Field tests, on the other hand, allowed the evaluation of system performance in more realistic scenarios, including both static configurations and dynamic situations involving moving vehicles. Under these conditions, it was possible to observe how factors such as node mobility, radio propagation, and environmental interference affect the performance of V2X communications. Overall, the experimental results

highlighted several relevant aspects. First, communication latency can increase significantly in the presence of interfering traffic, especially when the radio channel approaches saturation. Moreover, distributing traffic over different or adjacent channels may contribute to interference effects on the channel under analysis. These results confirm that the coexistence between IEEE 802.11p and C-V2X represents a significant technical challenge, particularly in high-traffic density scenarios. However, the adoption of appropriate channel switching mechanisms could help ensure efficient operation of both technologies. Such mechanisms may be implemented and optimized thanks to new Autotalks 350 chipsets, which will be capable of supporting both technologies simultaneously. Furthermore, the introduction of new multi-radio hardware solutions and the evolution of standards such as IEEE 802.11bd and NR-V2X could further improve performance and facilitate coexistence between different technologies. In conclusion, the work presented in this thesis provides an experimental contribution to the study of coexistence between IEEE 802.11p and C-V2X, highlighting the importance of realistic analyses based on hardware testing and real-world measurements. The obtained results represent a step toward a better understanding of V2X technology behavior in mixed scenarios and provide a useful foundation for future research in vehicular communications.

7.1 Future work

Several extensions of the work presented in this thesis are planned as future developments, both from an experimental perspective and in terms of the instrumentation used. First, thanks to the introduction of the Commsignia ITS-OB4, it will be possible to obtain more accurate latency measurements in message handling. Another possible extension concerns the evaluation of scenarios involving a larger number of vehicular nodes, with the goal of simulating more realistic traffic conditions and analyzing the behavior of V2X technologies in environments characterized by a higher communication density. Moreover, field tests will be repeated and averaged over a larger number of trials in order to build a more extensive dataset and reduce the statistical error resulting from a limited number of measurements. Further experimental campaigns will also consider messages of different sizes and transmission frequencies, in order to analyze how these parameters influence system performance in terms of latency and packet loss. Finally, regarding dynamic scenarios, it would be interesting to extend the analysis by considering vehicles moving at different speeds, in order to study the impact of mobility and radio propagation conditions on the performance of V2X communications.

Bibliography

[1] Marco Galvani. "History and future of driver assistance". In: *IEEE Instrumentation & Measurement Magazine* 22.1 (2019), pp. 11–16. DOI: 10.1109/MIM.2019.8633345 (cit. on p. 1).

[2] SAE International. *Taxonomy and Definitions for Terms Related to Driving Automation Systems for On-Road Motor Vehicles*. Revised April 2021, Issued January 2014. SAE International, Apr. 2021. DOI: 10.4271/J3016_202104. URL: https://doi.org/10.4271/J3016_202104 (cit. on p. 1).

[3] Francesco Raviglione. *Open Platforms for Connected Vehicles*. Tech. rep. Politecnico di Torino, Dec. 2022. URL: %7Bhttps://iris.polito.it/retrieve/8a1ec1bb-d525-4849-9a66-7a75c12ac87f/conv_phd_thesis_2022-v47-final_PDFA.pdf%7D (cit. on pp. 2, 6, 7, 13, 16, 19, 24, 29, 42, 44, 56).

[4] *Directive (EU) 2023/2661 of the European Parliament and of the Council of 22 November 2023 on type-approval of motor vehicles and engines and of systems, components and separate technical units intended for such vehicles, with respect to their emissions and battery durability, and on access to vehicle OBD information, repair and maintenance information, and vehicle cybersecurity, and repealing Regulation (EC) No 715/2007 and Regulation (EC) No 595/2009*. Official Journal of the European Union, L 2023/2661, 28.11.2023. ISSN 1977-0677 (electronic edition). 2023. URL: http://data.europa.eu/eli/dir/2023/2661/oj (cit. on p. 2).

[5] Lu Tao, Yousuke Watanabe, Yixiao Li, Shunya Yamada, and Hiroaki Takada. "Collision Risk Assessment Service for Connected Vehicles: Leveraging Vehicular State and Motion Uncertainties". In: *IEEE Internet of Things Journal* 8.14 (2021), pp. 11548–11560. DOI: 10.1109/JIOT.2021.3059222 (cit. on p. 2).

[6] Zuobin Ying, Maode Ma, and Longyang Yi. "BAVPM: Practical Autonomous Vehicle Platoon Management Supported by Blockchain Technique". In: *2019 4th International Conference on Intelligent Transportation Engineering (ICITE)*. 2019, pp. 256–260. DOI: 10.1109/ICITE.2019.8880167 (cit. on p. 3).

[7] Felipe Cunha, Leandro Villas, Azzedine Boukerche, Guilherme Maia, Aline Viana, Raquel A. F. Mini, and Antonio A. F. Loureiro. "Data communication in VANETs: Protocols, applications and challenges". In: *Ad Hoc Networks* 44 (2016), pp. 90–103. ISSN: 1570-8705. DOI: https://doi.org/10.1016/j.adhoc.

2016.02.017. URL: https://www.sciencedirect.com/science/article/pii/S1570870516300580 (cit. on p. 3).

[8] ETSI. *LTE; Service requirements for V2X services (3GPP TS 22.185 version 19.0.0 Release 19)*. Standard TS 122 185 V19.0.0. European Telecommunications Standards Institute, Oct. 2025 (cit. on p. 3).

[9] "On Multi-Access Edge Computing: A Survey of the Emerging 5G Network Edge Cloud Architecture and Orchestration". In: *IEEE Communications Surveys & Tutorials* 19.3 (2017), pp. 1657–1681. DOI: 10.1109/COMST.2017.2705720 (cit. on p. 5).

[10] Federal Communications Commission. *First Report and Order, Further Notice of Proposed Rulemaking, and Order of Proposed Modification – ET Docket No. 19-138*. Tech. rep. Federal Communications Commission, Oct. 2020. URL: %7Bhttps://docs.fcc.gov/public/attachments/DOC-367827A1.pdf%7D (cit. on p. 7).

[11] Junsung Choi, Vuk Marojevic, Carl B. Dietrich, Jeffrey H. Reed, and Seungyoung Ahn. "Survey of Spectrum Regulation for Intelligent Transportation Systems". In: *IEEE Access* 8 (2020), pp. 140145–140160. DOI: 10.1109/ACCESS.2020.3012788 (cit. on p. 7).

[12] Geeth P. Wijesiri N.B.A., Jussi Haapola, and Tharaka Samarasinghe. "A Discrete-Time Markov Chain Based Comparison of the MAC Layer Performance of C-V2X Mode 4 and IEEE 802.11p". In: *IEEE Transactions on Communications* 69.4 (Apr. 2021), pp. 2505–2517. ISSN: 1558-0857. DOI: 10.1109/TCOMM.2020.3044340 (cit. on p. 8).

[13] Rafael Molina-Masegosa, Javier Gozalvez, and Miguel Sepulcre. "Comparison of IEEE 802.11p and LTE-V2X: An Evaluation With Periodic and Aperiodic Messages of Constant and Variable Size". In: *IEEE Access* 8 (2020), pp. 121526–121548. DOI: 10.1109/ACCESS.2020.3007115 (cit. on p. 8).

[14] Waqar Anwar, Norman Franchi, and Gerhard Fettweis. "Physical Layer Evaluation of V2X Communications Technologies: 5G NR-V2X, LTE-V2X, IEEE 802.11bd, and IEEE 802.11p". In: *2019 IEEE 90th Vehicular Technology Conference (VTC2019-Fall)*. 2019, pp. 1–7. DOI: 10.1109/VTCFall.2019.8891313 (cit. on p. 8).

[15] 5GAA - 5G Automotive Association. *Coexistence of C-V2X and ITS-G5 at 5.9GHz*. Tech. rep. 5GAA, Apr. 2018. URL: https://5gaa.org/content/uploads/2018/10/Position-Paper-ITG5.pdf (cit. on p. 8).

[16] *V2X 350 Chip*. Accessed: 2026-02-18. URL: https://auto-talks.com/products/tekton3/ (cit. on p. 9).

[17] "IEEE Standard for Information Technology–Telecommunications and Information Exchange between Systems Local and Metropolitan Area Networks–Specific Requirements Part 11: Wireless LAN Medium Access Control (MAC) and Physical Layer (PHY) Specifications". In: *IEEE Std 802.11-2024 (Revision of IEEE Std 802.11-2020)* (2025), pp. 1–5956. DOI: 10.1109/IEEESTD.2025.10979691 (cit. on pp. 9–11).

[18] Chan Chi Fung, Sumendra Yogarayan, Siti Fatimah Abdul Razak, and Afizan Azman. "A Review Study of IEEE 802.11p On-Board Unit for V2X Deployment". In: *2023 11th International Conference on Information and Communication Technology (ICoICT)*. 2023, pp. 165–171. DOI: 10.1109/ICoICT58202.2023.10262808 (cit. on p. 9).

[19] Fabio Arena, Giovanni Pau, and Alessandro Severino. "A Review on IEEE 802.11p for Intelligent Transportation Systems". In: *Journal of Sensor and Actuator Networks* 9.2 (2020). ISSN: 2224-2708. DOI: 10.3390/jsan9020022. URL: https://www.mdpi.com/2224-2708/9/2/22 (cit. on p. 9).

[20] Yamen Y. Nasrallah, Irfan Al-Anbagi, and Hussein T. Mouftah. "Adaptive Backoff Algorithm for EDCA in the IEEE 802.11p protocol". In: *2016 International Wireless Communications and Mobile Computing Conference (IWCMC)*. 2016, pp. 800–805. DOI: 10.1109/IWCMC.2016.7577160 (cit. on p. 10).

[21] Christos Iliopoulos, Athanasios Iossifides, Chuan Heng Foh, and Periklis Chatzimisios. "IEEE 802.11BD for Next-Generation V2X Communications: From Protocol to Services". In: *IEEE Communications Standards Magazine* 9.2 (2025), pp. 88–98. DOI: 10.1109/MCOMSTD.2025.3569015 (cit. on pp. 11, 12).

[22] "IEEE Guide for Wireless Access in Vehicular Environments (WAVE) Architecture". In: *IEEE Std 1609.0-2019 (Revision of IEEE Std 1609.0-2013)* (2019), pp. 1–106. DOI: 10.1109/IEEESTD.2019.8686445 (cit. on p. 12).

[23] "IEEE Standard for Wireless Access in Vehicular Environments (WAVE) – Multi-Channel Operation". In: *IEEE Std 1609.4-2016 (Revision of IEEE Std 1609.4-2010)* (2016), pp. 1–94. DOI: 10.1109/IEEESTD.2016.7435228 (cit. on p. 12).

[24] *SAE International Technical Standard: V2X Communications Message Set Dictionary*. Revised September 2024. Issued December 2006. SAE International, 2024. DOI: 10.4271/J2735_202409. URL: https://doi.org/10.4271/J2735_202409 (cit. on p. 13).

[25] FCC -Federal Communications Commission. *SECOND REPORT AND ORDER AND SECOND FURTHER NOTICE OF PROPOSED RULEMAKING*. Tech. rep. FCC, Oct. 2025. URL: https://docs.fcc.gov/public/attachments/FCC-25-71A1.pdf (cit. on p. 13).

[26] Mario H. Castañeda Garcia, Alejandro Molina-Galan, Mate Boban, Javier Gozalvez, Baldomero Coll-Perales, Taylan Şahin, and Apostolos Kousaridas. "A Tutorial on 5G NR V2X Communications". In: *IEEE Communications Surveys & Tutorials* 23.3 (2021), pp. 1972–2026. DOI: 10.1109/COMST.2021.3057017 (cit. on pp. 15, 16).

[27] Jim Lansford. "LTE-V2X Technology and Standards". In: *2023 IEEE Conference on Standards for Communications and Networking (CSCN)*. 2023, pp. 73–76. DOI: 10.1109/CSCN60443.2023.10453158 (cit. on p. 15).

[28] Vittorio Todisco, Stefania Bartoletti, Claudia Campolo, Antonella Molinaro, Antoine O. Berthet, and Alessandro Bazzi. "Performance Analysis of Sidelink 5G-V2X Mode 2 Through an Open-Source Simulator". In: *IEEE Access* 9 (2021), pp. 145648–145661. DOI: 10.1109/ACCESS.2021.3121151 (cit. on p. 17).

[29] Mehdi Harounabadi, Dariush Mohammad Soleymani, Shubhangi Bhadauria, Martin Leyh, and Elke Roth-Mandutz. "V2X in 3GPP Standardization: NR Sidelink in Release-16 and Beyond". In: *IEEE Communications Standards Magazine* 5.1 (2021), pp. 12–21. DOI: 10.1109/MCOMSTD.001.2000070 (cit. on p. 17).

[30] Cheolkyu Shin, Emad Farag, Hyunseok Ryu, Miao Zhou, and Younsun Kim. "Vehicle-to-Everything (V2X) Evolution From 4G to 5G in 3GPP: Focusing on Resource Allocation Aspects". In: *IEEE Access* 11 (2023), pp. 18689–18703. DOI: 10.1109/ACCESS.2023.3247127 (cit. on p. 18).

[31] ETSI - European Telecommunications Standards Institute. *ETSI TS 103 836-5-1 V2.1.1 (2024-07) - Intelligent Transport Systems (ITS); Vehicular Communications; GeoNetworking; Part 5: Transport Protocols; Sub-part 1: Basic Transport Protocol; Release 2*. Tech. rep. ETSI, July 2024. URL: %7Bhttps://www.etsi.org/deliver/etsi_ts/103800_103899/1038360501/02.01.01_60/ts_1038360501v020101p.pdf%7D (cit. on pp. 18, 21).

[32] ETSI - European Telecommunications Standards Institute. *ETSI EN 303 613 V1.1.1 (2020-01) - IIntelligent Transport Systems (ITS); European profile standard for the physical and medium access control layer of Intelligent Transport Systems operating in the 5 GHz frequency band*. Tech. rep. ETSI, Jan. 2020. URL: %7Bhttps://www.etsi.org/deliver/etsi_en/303600_303699/303613/01.01.01_60/en_303613v010101p.pdf%7D (cit. on p. 18).

[33] ETSI TS 103 900 V2.2.1 (2025-02) - ETSI - European Telecommunications Standards Institute. *Intelligent Transport Systems (ITS); Facilities Layer; Cooperative Awareness Service; Release 2*. Tech. rep. ETSI, Feb. 2025. URL: https://www.etsi.org/deliver/etsi_ts/103900_103999/103900/02.02.01_60/ts_103900v020201p.pdf (cit. on p. 20).

[34] ETSI - European Telecommunications Standards Institute. *ETSI TS 103 831 V2.3.1 (2025-11) -Intelligent Transport Systems (ITS); Facilities Layer; Decentralized Environmental Notification Service; Release 2*. Tech. rep. ETSI, June 2023. URL: https://www.etsi.org/deliver/etsi_ts/103800_103899/103831/02.03.01_60/ts_103831v020301p.pdf (cit. on p. 20).

[35] ETSI - European Telecommunications Standards Institute. *ETSI TS 103 301 V2.2.2 (2024-11) -Intelligent Transport Systems (ITS); Vehicular Communications; Basic Set of Applications; Facilities layer protocols and communication requirements for infrastructure services; Release 2*. Tech. rep. ETSI, Nov. 2024. URL: https://www.etsi.org/deliver/etsi_ts/103300_103399/103301/02.02.02_60/ts_103301v020202p.pdf (cit. on pp. 20, 21).

[36] ETSI - European Telecommunications Standards Institute. *ETSI TS 104 091 V2.1.1 (2025-11) -InIntelligent Transport Systems (ITS);Facilities Layer; Services Announcement (SA) Service; Release 2*. Tech. rep. ETSI, Nov. 2025. URL: https://www.etsi.org/deliver/etsi_ts/104000_104099/104091/02.01.01_60/ts_104091v020101p.pdf (cit. on p. 20).

[37] ETSI - European Telecommunications Standards Institute. *ETSI TS 103 300-3 V2.3.1 (2025-12) -Intelligent Transport Systems (ITS); Vulnerable Road Users (VRU) awareness; Part 3: Specification of VRU awareness service; Release 2*. Tech. rep. ETSI, Dec. 2025. URL: https://www.etsi.org/deliver/etsi_ts/103300_103399/10330003/02.03.01_60/ts_10330003v020301p.pdf (cit. on p. 20).

[38] ETSI - European Telecommunications Standards Institute. *ETSI TR 103 562 V2.1.1 (2019-12) - Intelligent Transport Systems (ITS);Vehicular Communications;Basic Set of Applications; Analysis of the Collective Perception Service (CPS); Release 2*. Tech. rep. ETSI, Dec. 2019. URL: %7Bhttps://www.etsi.org/deliver/etsi_tr/103500_103599/103562/02.01.01_60/tr_103562v020101p.pdf%7D (cit. on p. 21).

[39] *Introduction to ASN.1*. Accessed: 2026-02-10. URL: https://www.itu.int/en/ITU-T/asn1/pages/introduction.aspx (cit. on p. 21).

[40] ETSI - European Telecommunications Standards Institute. *ETSI TS 103 248 V2.5.1 (2026-01) -Intelligent Transport Systems (ITS); GeoNetworking; Port Numbers for the Basic Transport Protocol (BTP); Release 2*. Tech. rep. ETSI, Jan. 2026. URL: https://www.etsi.org/deliver/etsi_ts/103200_103299/103248/02.05.01_60/ts_103248v020501p.pdf (cit. on p. 22).

[41] ETSI - European Telecommunications Standards Institute. *ETSI TS 103 836-3 V2.1.1 (2025-08) - Intelligent Transport Systems (ITS); Vehicular Communications; GeoNetworking; Part 3: Network Architecture; Release 2*. Tech. rep. ETSI, Aug. 2025. URL: %7Bhttps://www.etsi.org/deliver/etsi_ts/103800_103899/10383603/02.01.01_60/ts_10383603v020101p.pdf%7D (cit. on p. 22).

[42] ETSI - European Telecommunications Standards Institute. *ETSI TS 103 836-2 V2.1.1 (2024-07) - Intelligent Transport Systems (ITS); Vehicular Communications; GeoNetworking; Part 2: Scenarios; Release 2*. Tech. rep. ETSI, July 2024. URL: %7Bhttps://www.etsi.org/deliver/etsi_ts/103800_103899/10383602/02.01.01_60/ts_10383602v020101p.pdf%7D (cit. on p. 22).

[43] ETSI - European Telecommunications Standards Institute. *ETSI TS 103 836-1 V2.1.1 (2024-07) - Intelligent Transport Systems (ITS); Vehicular Communications; GeoNetworking; Part 1: Requirements; Release 2*. Tech. rep. ETSI, July 2024. URL: %7Bhttps://www.etsi.org/deliver/etsi_ts/103800_103899/10383601/02.01.01_60/ts_10383601v020101p.pdf%7D (cit. on p. 22).

[44] Mauro VITTORIO. *Serial Data Parsing for High-Fidelity GNSS Integration in ETSI C-ITS Vehicular Networks*. Tech. rep. Politecnico di Torino, Apr. 2025. URL: %7Bhttps://webthesis.biblio.polito.it/35761/1/tesi.pdf%7D (cit. on pp. 22, 23).

[45] Nikita Lyamin, Alexey Vinel, Dieter Smely, and Boris Bellalta. "ETSI DCC: Decentralized Congestion Control in C-ITS". In: *IEEE Communications Magazine* 56.12 (2018), pp. 112–118. DOI: 10.1109/MCOM.2017.1700173 (cit. on p. 24).

[46] ETSI - European Telecommunications Standards Institute. *ETSI TS 102 687 V1.2.1 (2018-04) - Intelligent Transport Systems (ITS); Decentralized Congestion Control Mechanisms for Intelligent Transport Systems operating in the 5 GHz range; Access layer part*. Tech. rep. ETSI, Apr. 2018. URL: %7Bhttps://www.etsi.org/deliver/etsi_ts/102600_102699/102687/01.02.01_60/ts_102687v010201p.pdf%7D (cit. on p. 24).

[47] ETSI - European Telecommunications Standards Institute. *ETSI TS 103 574 V1.1.1 (2018-11) - Intelligent Transport Systems (ITS);Congestion Control Mechanisms for the C-V2X PC5 interface; Access layer part*. Tech. rep. ETSI, Nov. 2018. URL: %7Bhttps://www.etsi.org/deliver/etsi_ts/103500_103599/103574/01.01.01_60/ts_103574v010101p.pdf%7D (cit. on p. 24).

[48] *Global Navigation Satellite System (GNSS)*. Tech. rep. PRINCETON UNIVERSITY. URL: %7Bhttps://www.etsi.org/deliver/etsi_ts/103500_103599/103574/01.01.01_60/ts_103574v010101p.pdf%7D (cit. on p. 25).

[49] Marco Rapelli, Francesco Raviglione, and Claudio Casetti. "OScar: An ETSI -Compliant C- ITS Stack for Field- Testing with Embedded Hardware Devices". In: *2024 22nd Mediterranean Communication and Computer Networking Conference (MedComNet)*. 2024, pp. 1–4. DOI: 10.1109/MedComNet62012.2024.10578207 (cit. on pp. 30, 32).

[50] Alessandro Bazzi, Alberto Zanella, Ioannis Sarris, and Vincent Martinez. "Co-channel Coexistence: Let ITS-G5 and Sidelink C-V2X Make Peace". In: *2020 IEEE MTT-S International Conference on Microwaves for Intelligent Mobility*

(ICMIM). 2020, pp. 1–4. DOI: 10.1109/ICMIM48759.2020.9299042 (cit. on p. 41).